

**USING OF NANOFIBER BASED  
ELECTRODES FOR DETECTION OF  
ORGANIC MOLECULES**

**ORGANİK MOLEKÜLLERİN TAYİNİ İÇİN  
NANOFİBER BAZLI ELEKTROTLARIN  
KULLANIMI**

**ANAERGULI MAIHEMUTİ**

**PROF. DR. NECDET SAĞLAM**  
Advisor

**ASSIST. PROF. DR. ÜMİT HAKAN YILDIZ**  
Co-Advisor

Submitted to Graduate School of Science and Engineering of  
Hacettepe University as a Partial Fulfillment of the Requirements  
for the Award of the Degree of Master of Science  
in Nanotechnology and Nanomedicine

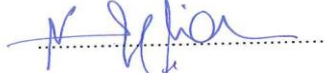
2018

This work named "**Using of Nanofiber based Electrodes for Detection of Organic Molecules**" by **ANAERGULI MAIHEMUTI** has been approved as a thesis for the Degree of **Master in Nanotechnology and Nanomedicine** by the below mentioned Examining Committee Members.

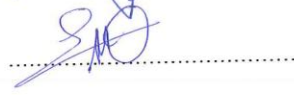
Prof. Dr. Hakan ATEŞ  
(Head)



Prof. Dr. Necdet SAĞLAM  
(Supervisor)



Assoc. Prof. Dr. Eylem GÜVEN  
(Member)



Assoc. Prof. Dr. Lokman UZUN  
(Member)



Assist. Prof. Dr. Mesut ŞAM  
(Member)



This thesis has been approved as a thesis for the **Master in Nanotechnology and Nanomedicine** by Board of Directors of the Institute for Graduate School of Science and Engineering.

Prof. Dr. Menemşe GÜMÜŞDERELİOĞLU  
Director of the Institute of  
Graduate School of Science and Engineering

## ETHICS

In this thesis study, prepared in accordance with the spelling rules of Institute of Graduate Studies in Science of Hacettepe University,

I declare that

- all the information and documents have been obtained in the base of academic rules
- all audio-visual and written information and results have been presented according to the rules of scientific ethics
- in case of using others Works, related studies have been cited in accordance with the scientific standards
- all cited studies have been fully referenced
- I did not do any distortion in the data set
- and any part of this thesis has not been presented as another thesis study at this or any other university.

14/06/2017



ANAERGULI MAIHEMUTI

## ÖZET

# ORGANİK MOLEKÜLLERİN TAYİNİ İÇİN NANOFİBER BAZLI ELEKTROTLARIN KULLANIMI

**Anaerguli MAIHEMUTİ**

**Yüksek Lisans, Nanoteknoloji ve Nanotıp Anabilim Dalı**

**Tez Danışmanı: Prof. Dr. Necdet Sağlam**

**Tez Eş Danışmanı: Dr. Öğr. Üyesi Ümit Hakan Yıldız**

**Haziran 2018, 80 sayfa**

Ülkemizde kullanılan diyabet sensörlerinin kullan-at formundaki elektrotları, ithal edilme zorunluluğu nedeniyle dışa bağımlılık oluşturmaktadır. Ayrıca bu tip elektrotlar, sadece kandaki glukozu ölçebilecek duyarlılıkta olup, diğer analitlerin ölçümü için kullanılmaktadır. Etanol, metanol ve glukoz seviyelerinin tayini için, yüksek duyarlılıkta ve seçicilikte elektrotların geliştirilmesi zorunlu hale gelmiştir.

Son derece küçük çap ölçüleri nedeniyle, yüksek yüzey/hacim oranına sahip olan elektrodeğirilmiş nanolifler, aynı zamanda yapısal olarak sağlam ve esnek yapılardır. Bu özelliklerine bağlı olarak, elektrodeğirilmiş nanolifler, biyomolekül tespiti için uygun malzemelerdir ve enzim tabanlı biyosensör uygulamalarında sıklıkla kullanılmaktadırlar. Bu tez çalışması, organik polimer nanolif – karbon nanotüp (CNT) nanokompozit malzemelerin glukoz biyosensör uygulamasını içermektedir. Bu çalışmada, yeni bir yaklaşımla yüzey aktif nanolif malzemelerin sentezi ve bu malzemelerin elektrokimyasal sensör platformunda kullanılması araştırılmıştır. Çalışmada, glukoz oksidaz ve alkol oksidaz enzimleri kullanılarak farklı beş sensör elektrodunun, glukoz, metanol ve etanol algılama aktivitelerine göre karşılaştırmalı

olarak çalışılması amaçlanmıştır. Fakat glukoz oksidaz temelli amperometrik enzim elektrotları, kan şekeri testi için basit, kullanımı kolay sistemler arasında başı çekmektedir ve glukozun devamlı izlenmesinde önemli bir rol oynadığı düşünülmektedir. Bu sebeplerden dolayı ve laboratuvar koşullarımızın kısıtlı olmasından ötürü, çalışmamızda yalnızca glukoz oksidaz enzimi kullanılmıştır.

Çalışma sırasında geliştirilen elektrotlar: a) Glukoz oksidaz (GOks) içeren elektroeğirilmiş PVA elektrot; b) Glukoz oksidaz (GOks)-Çok katmanlı karbon nanotüp (MWCNT) içeren elektroeğirilmiş PVA elektrot; c) Glukoz oksidaz (GOks) ve poli dialil dimetil amonyum klorür (PDDA) ile modifiye edilmiş çok katmanlı karbon nanotüp (MWCNT) içeren elektroeğirilmiş PVA elektrot; d) Glukoz oksidaz (GOks)-poli dialil dimetil amonyum klorür (PDDA) ile modifiye edilmiş tek katmanlı karbon nanotüp (SWCNT) içeren elektroeğirilmiş PVA elektrot; e) Arayüzey çapraz bağlanmış ve Glukoz oksidaz (GOks)-poli dialil dimetil amonyum klorür (PDDA) ile modifiye edilmiş çok katmanlı karbon nanotüp (MWCNT) içeren elektroeğirilmiş PVA elektrot olarak hazırlanmıştır. Elektroeğirme tekniği ile organik bazlı bazı polimerler kullanılarak üretilen nanofiberlerden elektrot üretimi gerçekleştirilmiştir.

Elektroeğirme nanoliflerin fiziksel morfolojisi ve ortalama çap uzunlukları, taramalı elektron mikroskopu (SEM) kullanılarak incelenmiş olup, nanoliflerin ortalama çap uzunluğu 100 nm olarak belirlenmiştir. Elektrotların glukoz algılama aktiviteleri amperometrik olarak -0.5 V potansiyel fark uygulanarak, 0.1 M fosfat tampon çözeltisi (PBS, pH 7.4) içerisinde gerçekleştirilmiştir. Üretilen c-d sensör elektrotlarının glukoz algılama limitleri 0.024 mM olarak, glukoz algılama hassasiyetleri ise sırasıyla 65.8, 42.7  $\mu\text{AmM}^{-1}\text{cm}^{-2}$  olarak tespit edilmiştir ve glukoz tayini için son kullanıma uygun sensör elektrotları olarak değerlendirilmiştir. Üretilen a-b-e sensör elektrotlarının glukoz algılama limitleri sırasıyla 0.048, 0.048 ve 0.12 mM olarak, glukoz algılama hassasiyetleri ise sırasıyla 19.4, 25.9, 4.01  $\mu\text{AmM}^{-1}\text{cm}^{-2}$  olarak tespit edilmiştir.

**Anahtar Kelimeler:** Elektroeğirme, nanofiber, nanobiyosensör, karbon nanotüp

## **ABSTRACT**

### **USING OF NANOFIBER BASED ELECTRODES FOR DETECTION OF ORGANIC MOLECULES**

**Anaerguli MAIHEMUTI**

**Master of Science, Nanotechnology and Nanomedicine Division**

**Advisor: Prof. Dr. Necdet Sağlam**

**Co-Advisor: Assist. Prof. Dr. Ümit Hakan Yıldız**

**June 2018, 80 pages**

The disposable electrodes of the diabetes sensors used in our country are in the case of external dependency due to the necessity of importation. In addition, these types of electrodes are only capable of measuring the glucose in blood, and are using for the measurement of other analytcs. Consequently, it has become compulsory to develop electrodes with the characteristics of high sensitivity and selectivity for the determination of ethanol, methanol and glucose levels.

Electrospun nanofiber membranes are structurally sound and flexible materials. The membranes are promising candidates for immobilization of enzymes because of their high specific surface area and porous structure. A novel technique for designing amperometric glucose biosensor by electrospinning poly (vinyl alcohol) (PVA) - carbon nanotube (CNT) nanocomposite materials is presented in this study. It was aimed to investigate glucose, ethanol and methanol detection efficiency of five different enzyme electrodes using alcohol oxidase and glucose oxidase enzymes by manipulating the structural design and composition of nanocomposite membranes. However, Glucose oxidase-based enzyme electrodes are among the simplest, easy-to-use systems for blood sugar testing and play an

important role in the continuous monitoring of glucose. Because of these reasons and due to our limited laboratory conditions, glucose oxidase was selected and immobilized onto the surface of sensor electrodes.

The electrodes developed in this study were prepared as: a) Glucose oxidase (GOx) immobilized PVA electrospun electrode; b) Glucose oxidase (GOx) immobilized PVA electrospun electrode containing multi-walled carbon nanotube (MWCNT); c) Glucose oxidase (GOx) immobilized PVA electrospun electrode containing poly(diallyldimethylammonium chloride) (PDDA) functionalized multi-walled carbon nanotube (MWCNT); d) Glucose oxidase (GOx) immobilized PVA electrospun electrode containing poly(diallyldimethylammonium chloride) (PDDA) functionalized single-walled carbon nanotube (SWCNT); e) Interfacially cross-linked PVA electrospun electrode containing poly(diallyldimethylammonium chloride) (PDDA) functionalized multi-walled carbon nanotube (MWCNT). Poly(vinyl alcohol) (PVA)/Glucose oxidase (GOx)/graphene biocomposite membranes were prepared using an electrospinning technique and used for enzyme immobilization.

The PVA/GOx membrane's morphology was examined by scanning electron microscopy (SEM). Average diameter for the neat PVA electrospun nanofibers were observed as 100 nm. Glucose sensing activities of the electrodes were amperometrically measured at an applied voltage of -0.5 V (vs. Ag/AgCl) in 0.1 M phosphate buffer solution (PBS pH 7.4). Amperometric measurements demonstrated that electrospun fibrous enzymatic electrodes glucose detection limits for (c) and (d) sensor electrode was observed as 0.024 mM and the glucose sensitivity were calculated as 65.8 and 42.7  $\mu\text{AmM}^{-1}\text{cm}^{-2}$ , respectively. Glucose detection limit and sensitivity of these sensor electrodes are quite satisfying. Glucose detection limits of the fabricated glucose electrodes (a), (b), and (e) were observed as 0.048, 0.048 and 0.12 mM respectively, and calculated glucose sensitivity of these sensor electrodes were 19.4, 25.9, 4.01  $\mu\text{AmM}^{-1}\text{cm}^{-2}$ , respectively.

**Keywords:** Electrospin, nanofiber, nanobiosensor, carbon nanotube

## **ACKNOWLEDGE**

By the end of this work, I want to firstly thank to my family for their great support and motivation during all the period. I also want to thank to all the friends who have helped me during the experimental period and treated me how to use all the instruments inside and outside of the laboratory. At the same time, I thanks to the PhD student Ezgi Emül from the laboratory of Prof. Dr. Necdet Sağlam who made me work with a high level of comfortable and huge amount of support, always with a smile faces and respectful attitude.

At the same time, I want to sincerely thank to my supervisor Prof. Dr. Necdet Sağlam in Hacettepe University for his great encouragement and guiding from the very beginning till the end of this period with his knowledge and experience, and co-supervisor Assist. Prof. Ümit Hakan Yıldız in İzmir Institute of Technology for his huge amount of support and help on solving my problems during all the experimental period in his laboratory.

Finally, I want to thank to the committee member of my thesis for their discussion and examination during my thesis presentation.



# TABLE OF CONTENTS

	<u>Page</u>
ÖZET .....	IV
ABSTRACT .....	II
ACKNOWLEDGE .....	IV
TABLE OF CONTENTS .....	V
LIST OF FIGURE .....	VIII
LIST OF TABLES .....	XI
LIST OF ABBREVIATION .....	XII
1. INTRODUCTION.....	1
2. GENERAL INFORMATION .....	5
2.1. Overview of Electrospinning.....	5
2.2. Structure and morphologies of polymeric nanofibers .....	7
2.2.1. Applied voltage .....	7
2.2.2. Tip collector distance .....	7
2.2.3. Flow rate of polymer .....	7
2.2.4. Spinning environment .....	7
2.2.5. Concentration of solution .....	8
2.2.6. Solution conductivity. ....	8
2.2.7. Volatility of solvent .....	8
2.3. Carbon nanotubes (CNTs) .....	8
2.3.1 Characterization of Carbon nanotubes (CNTs).....	9
2.4. Enzyme immobilization .....	10
2.4.1. Non-covalent enzyme immobilization.....	11
2.4.2. Covalent Linking .....	13
2.5. Glucose Oxidase Immobilization .....	13
2.5.1. Glucose Oxidase Properties .....	14

2.5.2. Glucose Oxidase Reaction Mechanism .....	14
2.5.3. Glucose Oxidase Activity Analysis .....	16
2.6. Alcohol Oxidase Immobilization .....	17
2.6.1. Properties and Application of Alcohol Oxidase .....	17
2.6.2. Alcohol Oxidase Reaction Mechanism.....	18
2.6.3. Alcohol Oxidase Activity Analysis .....	20
2.7. Polyvinyl Alcohol (PVA).....	21
2.7.1. Properties and Application of PVA .....	22
2.7.2. Cross-linking of PVA .....	23
2.8. Scanning Electrochemical Microscopy (SECM) Analysis.....	24
3. EXPERIMENTAL SECTION.....	26
3.1. Materials .....	26
3.2. Methods .....	26
3.3. Pretreatment of SWCNTs and MWCNTs .....	27
3.4. Preparation of CNTs Modified PVA Nanofiber Membrane .....	27
3.4.1. PVA Coating of Pencil Graphite Electrode .....	28
3.5. Preparation of Cross-linking PVA Electrospun Membranes .....	30
3.6. Interfacial Cross-linking of PVA Nanofiber Mat .....	30
3.7. Preparation of CNT- (PDDA/GOx) <sub>2</sub> Conjugate.....	30
3.8. Electrochemical measurements .....	32
3.8.1. Electrochemical measurements of GOx.....	32
4. RESULTS AND DISCUSSION .....	34
4.1. PVA Electrospun Nanofibers Characterization.....	34
4.2. PVA coating of pencil graphite electrode .....	38
4.3. Electrochemical Characterization.....	40
4.4 Characterization of PVA/CNT composite nanofiber mats.....	43
4.5. Enzyme Electrodes .....	45

4.5.1. Glucose sensing activities of the enzyme electrodes.....	45
5. CONCLUSIONS.....	55
REFERENCES.....	57
CURRICULUM VITAE.....	63



## LIST OF FIGURE

	<u>Page</u>
Figure 2.1. Electrospinning setup in our laboratory .....	5
Figure 2.2. Schematic of electrospinning process [26] .....	6
Figure 2.3. Schematics of SWCNTs and MWCNTs [38] .....	9
Figure 2.4. Oxidation of CNTs in strong acidic conditions [40] .....	10
Figure 2.5. Schematic illustration of different type of enzyme immobilization methods [29]. .....	11
Figure 2.6. Physical absorption of enzyme on CNTs [45]. .....	12
Figure 2.7. Representation of glucose oxidase immobilization on SWNTs surface of by layer-by-layer immobilization technique. PSS: poly (sodium 4-styrenesulfonate); IL: ionic liquid with permission [49] .....	13
Figure 2.8. Illustration of Glucose oxidase catalysis reaction [53] .....	15
Figure 2.9. Schematic illustration of two different mechanisms proposed for reductive half-reaction [53]. .....	15
Figure 2.10. Schematic illustration of GOx reaction with ABTS [55]. .....	16
Figure 2.11. Schematic illustration of GOx reaction with chromagenic dye o-dianisidine [56]. .....	17
Figure 2.12. Schematic representation of Alcohol oxidase catalyzes .....	19
reaction [58]. .....	19
Figure 2.13. Schematic representation of a) Alcohol dehydrogenase (ADH) as catalyst, b) alcohol oxidase (AOX) as catalyst [59]. .....	19
Figure 2.14. Schematic representation of a) Alcohol oxidase (AOD) reaction with chromagenic dye o- dianisidine, and b) Alcohol oxidase reaction with ABTS21	
Figure 2.15. The illustration of chemical structure of PVA and vinyl alcohol B: PVA is synthesized [61]. .....	22
Figure 2.16. Mechanism of cross-linking reaction between PVA and GA [65]. .....	24
Figure 2.17. Scanning electrochemical microscopy working principle. (a) By using	

the UME far, (b) Diffusion on an Insulating substrate, (c) Diffusion on a conductor, and the mediators are generated again [66].....	25
Figure 3.1. Typical electrospinning set up in our laboratory .....	29
Figure 3.2. Schematic illustration of pencil graphite electrode fiber coating set up with stable coating system [68] .....	29
Figure 3.3. Schematic representation of CNT-(PDDA/GOx/AOx) <sub>2</sub> conjugate preparation steps [49]. .....	31
Figure 3.4. Schematic representation of batch and flow-injection cells used for dual amperometric measurements [67]. .....	33
Figure 4.1. a) SEM image of 10 wt% PVA, b) Photographic image of PVA nanofibers, c) PVA electrospun nanofibers fiber diameter distribution.....	35
Figure 4.2. SEM image cross-linked PVA nanofibers and the fiber diameter distribution a) 1h, b) 3h, c) 24 h .....	36
Figure 4.3. ATR FT-IR spectrum of PVA cross-linked nanofibers, a)3 h, b) 24 h, c) 1 h, d) neat PVA nanofibers.....	38
Figure 4.4. Photographic image of a) bare pencil graphite electrode, b) PVA coated pencil graphite electrode .....	39
Figure 4.5. SEM micrograph of 1 min (a), 2 min (b) and 5min (c) coating of pencil graphite electrode .....	39
Figure 4.6. Correlation between PVA spinning time and fiber coating thickness on the surface of electrode. ....	40
Figure 4.7. Cyclic voltammograms of PVA nanofiber coated pencil graphite electrode and bare pencil graphite electrode in 50 mM Fe(CN) <sub>6</sub> <sup>3-/4-</sup> in 1 mM potassium chloride.....	41
Figure 4.8. Correlation between the fiber mat thickness, coating time and peak current.....	42
Figure 4.9. Electrochemical Impedance Spectra of PVA coated pencil graphite electrode and bare pencil graphite electrodes in 10 mM Fe(CN) <sub>6</sub> <sup>3-/4-</sup> solution in 0.2 mM potassium chloride.....	43
Figure 4.10. Cyclic voltammograms of bare PGE, PVA electrospun nanofiber	

coated PEG, PVA/MWCNT-PEG and interfacial cross-linked PVA/MWCNT-PEG. ....	44
Figure 4.11. a) Chronoamperometric response of GOx bare pencil graphite electrode for the successive injection of 1mM glucose in a stirred 0.1 M PBS (pH 7.4) with -0.5 V Potencial, b) correlation between glucose concentration and current response, c) Calibration curve.....	46
Figure 4.12. a) Chronoamperometric response of GOx immobilization of PVA electrospun electrode for the successive injection of 1mM glucose in a stirred 0.1 M PBS (pH 7.4) with -0.5 V Potencial, b) correlation between glucose concentration and current response, c) Calibration curve. ....	47
Figure 4.13. a) Chronoamperometric response of GOx immobilized PVA electrospun electrode modified with MWCNT for the successive injection of 1mM glucose in a stirred 0.1 M PBS (pH 7.4) with -0.5 V Potencial, b) correlation between glucose concentration and current response, c) Calibration curve.....	49
Figure 4.14. a) Chronoamperometric response of GOx immobilized PVA electrospun electrode functionalized with MWCNT/PDDA for the successive injection of 1mM glucose in a stirred 0.1 M PBS (pH 7.4) with -0.5 V Potencial, b) correlation between glucose concentration and current response, c) Calibration curve. ....	50
Figure 4.15. a) Chronoamperometric response of GOx immobilized PVA electrospun electrode functionalized with SWCNT/PDDA for the successive injection of 1mM glucose in a stirred 0.1 M PBS (pH 7.4) with -0.5 V Potencial, b) correlation between glucose concentration and current response, c) Calibration curve.....	51
Figure 4.16. a) Chronoamperometric response of Interfacially cross-linked PVA electrospun electrodecontaining PDDA functionalized MWCNT at an applied Potential of -0.5 V to succesive addition of 1mM glucose in a stirred 0.1 M, pH 7.4 PBS, b) Relationship between curve.....	52

## LIST OF TABLES

	<u>Page</u>
Table 1.1. Diabetes patients growing problem all over the world .....	2
Table 4.1. Characteristics of before and after cross linking of PVA nanofibers. ....	37
Table 4.2. Calculated sensitivities of five different enzyme electrodes.	<b>Error! Bookmark not defi</b>



## LIST OF ABBREVIATION

PVA	polyvinyl alcohol
CNT	carbon nanotube
GOx	glucose oxidase
SWCNT	single-walled carbon nanotube
MWCNT	multi-walled carbon nanotube
PDDA	poly (diallyldimethylammonium chloride)
PGE	pencil graphite electrode
CV	Cyclic voltammetry
ABTS	2,2'-Azino-di-[3-ethylbenzthiazolin-sulfonate]
FAD	flavin adenine dinucleotide
PVAc	polyvinyl acetate



# 1. INTRODUCTION

The ideas of “The possibility to create nano-sized products with the use of atoms as building particles” was mentioned for the first time in 1959 by Mr. R. Feynman as “There is a lot of space down there”. In 1974, and after that the word of “nanotechnology” was mentioned firstly by N. Taniguchi to scientific world. At one of the international conference held in Tokyo about industrial production, his description of superthin processing and nano-sized mechanism creation. And in 1986, the idea mentioned by Feynman was written firstly in a named "Vehicles of creation: the arrival of the nanotechnology era" by E. Drexler. A considerable intensification of nanotechnological researches and discoveries is in progression, and numbers of publications related to nanotechnology are sharply increasing since the second half of 1980s to the early 1990s [1].

Nanotechnology has led to a dramatic improvement in biosensors, and contributed greatly in making biosensors more effective and applicable. The nanotechnology based biosensor is revolutionizing the health care industry as a biosensor used in detecting of diabetes and testing of metabolites etc [2].

Nanomaterials are a special gift of nanotechnology to the humanbeings, which are the materials with 1-100 nm sized and are intended to be used in producing biosensors. The size makes the materials very special as they have unique properties which is not present in their corresponding bulk forms [3] Several nanomaterials including nanotubes, nanowires, nanorods, nanoparticles and thin films have been investigated for using in nanobiosensors as a transduction mechanisms and biological signaling [4] With the advantages of nanobiosensors technology and its unique impact on manufacturing ultrasensitive, ultra-selective and economic devices, application of nanobiosensors are enhanced significantly in the area of medical diagnostics, environmental protection and etc. Diabetes is a metabolic disorder that causes 4 million deaths every year and there are more than 170 million diabetes all over the world. The cells of the people suffered from diabetes need insulin for adsorbing blood sugar (glucose), and they suffer from shortage of glucose when the level of glucose build up in blood. If the diabetes is not treated or is not properly managed, the high level of glucose in blood can

slowly damage both large and small blood vessels and hereby results in a diversity of complication [5]. Furthermore, over the past 5 years, the percentage of the disease has risen with an alarming 11%, and new cases with further doubling is estimated by WHO (2004) in the next 25 years (Table 1.1).

Table 1.1. Diabetes patients growing problem all over the world

Statistics	1995	2000 (estimated)	2025 (estimated)
Diabetes patients	135	154	300
Female / Male %	25.2	23.8	17.1
In developed countries	1.18	1.16	1.12

Due to the critical importance of continuously measuring the level of glucose in blood, it has become necessary to develop biosensors that can accurately detect the level of ethanol, methanol and glucose in blood with high sensitivity and selectivity for personal and clinical diagnosis [6].

Different methods for determination of ethanol/methanol/glucose have been developed that including chemiluminescence, optical, acoustic, nanogels under fluorescent, field effect transistors, near infrared spectroscopy and approaches of transdermal [7]. However, these technologies need expensive and more complicated designing for devices, and by contrast with this, electrochemical biosensor technologies have significant properties of low cost, and easy to use as well as fabrication of miniaturization for portable sensing device with high sensitivity, high selectivity and lower response time [8].

Electrochemical biosensors are available in two different forms such as enzymatic biosensor and non-enzymatic biosensor. The enzymatic procedure is the most preferred due to the unique properties on eliminating the use of hazardous chemicals and improving the procedure selectivity [9]. Enzymes generally have been immobilized on the surface of solid support for improving the stability of enzymes [10]. As for supporting materials, the nanomaterials have gain a significant attention due to their unique properties, besides, the electrode surface

of biosensors with nano-scale design controls the structure of these nanomaterials [11].

Nanofibers are fiber structured materials, which have unique physical and mechanical properties because of their high surface area versus volume ratio. The electrospun fibers with extremely small diameter measurements less than 100 nm, have variety of applications in different field of areas such as food products, energy storage, transistors, aerospace medical and drug delivery system with their structurally sound and flexible properties [12]. Depending on these properties, electrospun nanofibers are suitable materials for biomolecule detection and are frequently used in enzyme based biosensor applications. Various micro and nanometer-sized polymer fibers are frequently used in textile composites, tissue engineering applications, sensors, catalysis, drug release systems, and high-performance membrane filter systems [13]. For fabricating these highly porous structures, various methods are used such as fiber bonding, solvent casting, particle leaching, phase separation, emulsion freeze drying, gas foaming and 3-D printing techniques [14]. Despite all these different methods, the ease of electrospinning technology offers attractive advantages for the scaffold structure. Structures produced by electrospinning technique have significant characteristics such as morphologically similar to natural tissues, and have high surface area per unit mass due to their extremely small diameters. These unique features of this technique made it more preferred. In addition, it is inevitable that the electrospinning fibers increase the affinity of the membrane filter to be formed by the static charge, and therefore become the first priority technique for the structures to be developed in the field of filtration [15].

Electrospinning technique was firstly observed in 1897 by Rayleigh and deeply examined by Zelenny in 1914 about electro spraying and after that it was patented by Formhals Anton with his published patents related to a process and an apparatus for the production of artificial filaments with the Patent Number: 1,975,504,1934 [16].

In the past 60 years, nearly 50 patents have been published in the field of electrospinning polymer fibers [17]. Since the 1980's, electrospinning technique has increased the curiosity of researchers due to particularly due to the surging interests to the submicron and nanometer-sized ultra-fine fiber structures [18]. At

the present time, approximately 200 research institutes and universities are doing researches on electrospinning process [19].

Since the 1990's, many groups have been working on materials developed by electrospinning technique, which are used in the areas of biomedical, electronics, textile and filtration. Different ingredients were obtained from various organic and inorganic materials by using electrospinning technique [20] [21] [22].



## 2. GENERAL INFORMATION

### 2.1. Overview of Electrospinning

Electrospinning is a technique to fabricate electrospun nanofibers with diameters from 2 nm to some micrometers by applying electrical forces to the prepared solution of polymer [23]. In the process of electrospinning, high voltage source is used to form the polymer jet which is electrically charged. The electrically charged jet is placed in a glass tube or a syringe. The injector is connected to a syringe piston to allow fluid to flow at a constant rate.



Figure 2.1. Electrospinning setup in our laboratory

A basic electrospinning process including three important components such as high voltage power supply, ground metal collector and a micro-infusion pump. Figure 2.1. shows an electrospinning setup.

One of the electrodes is connected to the collector, and the other one is connected to the tip of the injector contains the spin solution. The electric field is used to the tip of the injector with polymeric solution. There is a load on the liquid surface. This results in an opposite force to the surface tension between polymeric liquid and the capillary tube.

As the electric field intensity increases, the charged surface of prepared polymer solution forms a conical drop that is generally known as "Taylor cone" at the tip of the capillary tube. The Taylor's concept provides a balance among electric field and polymer surface tension. A defined value is reached when the electrostatic forces overcome the droplet surface tension, a jet formed polymer ejected from the droplet then collected as nanofibers to the surface of charged jet collector [25]. Figure 2.2. shows electrospinning of nanofibers process.

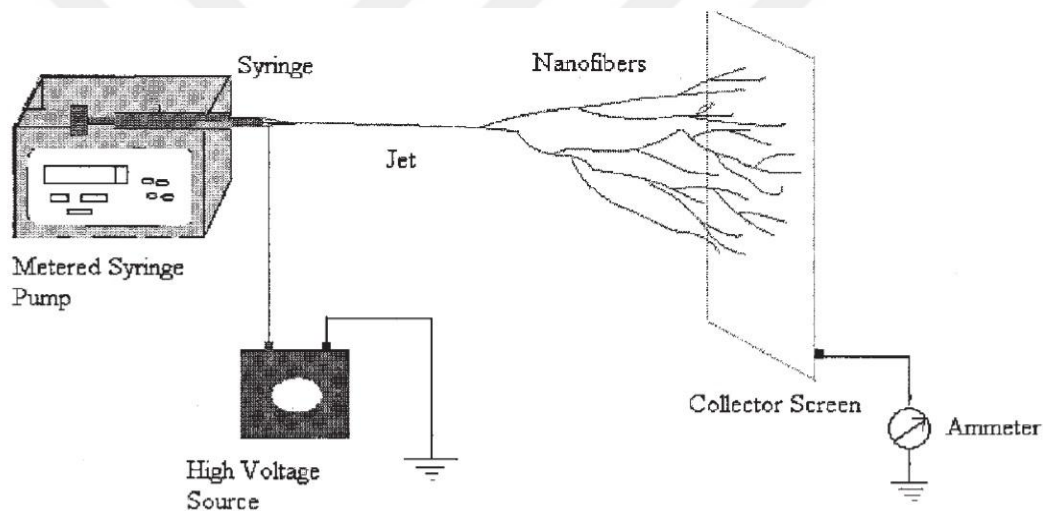


Figure 2.2. Schematic of electrospinning process [26]

The advantage of nanofiber membranes is their high ratio of surface to the volume, high porosity and low pore diameter. Because of the reasons, it is expected that the membranes prepared with the nanofiber structure should have a higher heavy metal absorption capacity [27].

## **2.2. Structure and morphologies of polymeric nanofibers**

Nanofibers produced by electrospinning process is affected directly by the polymers viscoelastic behavior and applied electrical voltage. The structure and characteristics of nanofibers is affected by different parameters during the fiber spinning process such as applied voltage, solution feed rate, spinning environment like humidity and temperature, distance between the nozzle and collector, characteristics of the materials like surface tension, concentration of the solution, conductivity, viscosity and vapor pressure of the solvent [28].

### **2.2.1. Applied voltage**

In the process of electrospinning, because of the voltage applied, the charge transport originates mainly from the polymer jet flowing towards the collector. The mass flow of the polymer from the syringe tip towards collector is referred by the increase or decrease of the spinning current. As researched by Deitzel et al, applied voltage increment raise the rate of deposition because of the higher flow rate from the tip, and also influences the morphology and structure of polymer nanofibers and changes the jet starting point shape [29].

### **2.2.2. Tip collector distance**

The distance between collector and syringe tip always affects the structure and morphology of electrospun nanofibers due to the dependence of evaporation rate, imbalance interval and deposition time. A decrease in tip-collector distance fabricates wet fibers and beaded structures while regardless of solution concentration. And the fiber morphology also changes its shape to straight from round [30].

### **2.2.3. Flow rate of polymer**

Polymer solutions flow rate from the injector is an important parameter as it can affect polymer transporting rate and spraying rate. It has been observed that, an increment in the flow rate of polymer from the syringe results enhanced pore diameter and fiber diameter, and the fibers had showed beaded morphologies [31].

### **2.2.4. Spinning environment**

Different electrospinning environments like vacuum condition, surrounding gas, humidity of the surrounding air influences the fiber structure and morphology. It

has been studied that acrylic fibers which was fabricated under air condition at which the relative humidity higher than 70% could not be dried appropriately and become entwined at the collector surface [32].

#### **2.2.5. Concentration of solution**

The concentration of solution always controls the limiting borders for fabricating fibers because of the diversities in the surface tension and viscosity. As it studied by researchers, surface tension affects the low concentration solution to form droplet while higher viscosity forbidding the higher concentration solution fiber formation [33]. As is evident from the studies, higher polystyrene solution concentration results in higher fiber diameter lower pore size.

#### **2.2.6. Solution conductivity.**

Most of the polymers are conductive and the charged ions plays critical role during the process of jet formation. After that ions from polymeric solution raise the charge transferring capability of the jet and exposing it to rather high tension by electric field applied in the fabricating process [34].

#### **2.2.7. Volatility of solvent**

Solvent volatility has a major role in producing fiber structure with its effect on the process of phase separation. It has been studied that higher solvent volatility results the morphologies with nano and microstructure while lower solvent volatility results in a microstructure which is much-diminished [32].

### **2.3. Carbon nanotubes (CNTs)**

Carbon nanotubes (CNTs) firstly reported by Sumio in 1991. These materials are formed of rolling graphene sheets, and exhibits a structure with nanometer in diameter and microns for length. CNTs demonstrate different field of application because of their unique characteristics such as structural, optical, electrical and thermall properties [35]. These materials with application potentials, having been used in the field of chemical and biological sensor applications, chemical energy storage, nanotransistors and emission arrays. The basic point of these applications is to develop more functional composite materials by supporting with carbon nanotubes. Carbon nanotube based electrochemical sensors are mostly preferred as they have high sensitivity and excellent mechanical properties.



Carbon nanotubes deposited on thin membranes, which is used in gas sensor applications, allow both selective gas determination and trace amount of gas analysis at low concentrations [36]. Carbon nanotubes, which are extremely efficient in gas sensor applications, can also exhibit the same performance in aqueous solutions detections just after the surface modification in an effective method.

### 2.3.1 Characterization of Carbon nanotubes (CNTs)

Carbon nanotubes have two main types such as multi-walled carbon nanotubes(MWCNTs) and single-walled carbon nanotubes. SWCNTs (0.75-3 nm in diameter) have one layer rolling graphene sheet while multi-walled carbon nanotubes (2-100 nm in diameter) have more than two layer of rolling graphene sheet, and the distance between each graphene layer is about 0.42 nm [37]. The structure of SWCNTs and MWCNTs are represented respectively in Figure 2.3.

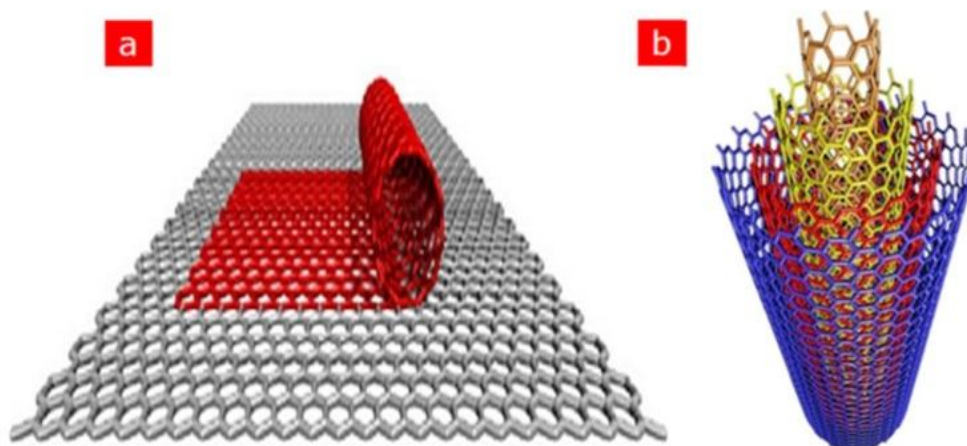


Figure 2.3. Schematics of SWCNTs and MWCNTs [38]

It has been confident that, CNTs can be purified by two different methods. One is to control catalysts concentration in feedstock. When the concentration of catalysts decreased, resulting impurities also decrease. The other method is to purify carbon nanotubes by acid treatment [39]. Acid treatment is a popular and most-known process for CNTs purification. The oxidation of CNTs in acidic conditions is showing in Figure 2.4.

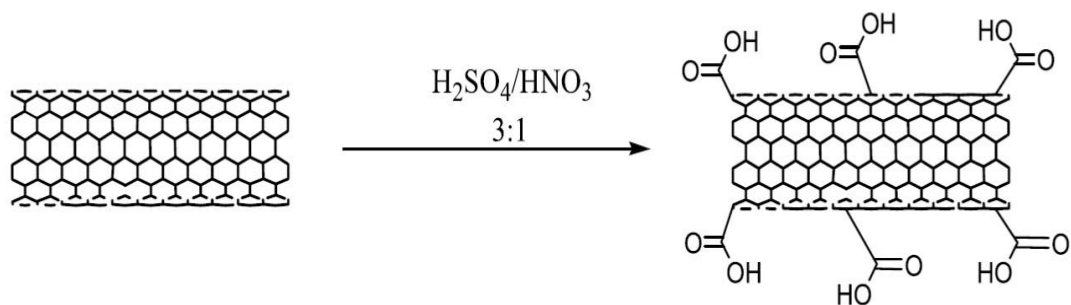


Figure 2.4. Oxidation of CNTs in strong acidic conditions [40]

However, the CNT wall structures can be damaged during the acid treatment process, and developing different kinds of functional groups like carbonyl, phenol and carboxylic acid [41]. These shortages influencing the strength of CNT fibers. To avoid these disadvantages of acid treatment, functional groups can be used for cross-linking reaction. It has been researched that using covalent cross-linking bonds between individual carbon nanotubes resulted in increased strength of carbon nanotube fiber due to the cross-linking bonds assists poor shear interactions [42].

#### 2.4. Enzyme immobilization

Immobilization of enzymes onto different matrix or surface has been broadly studied [43]. Enzymes and other immobilized biomolecules often demonstrate significant and improved capacity to be used again once after immobilized onto a different surface or material surface. Immobilized enzymes or biomolecules represent great properties with its soluble form, because there is no need to continually repair the protein catalyst besides the effortless on eliminating the enzymatic components after the reactions. All of these favorable advantages can beat a path for higher processing efficiency and low funding costs for enzymes used in industrial systems. Different methods for immobilizing enzymes (Figure 2.5) on to organic or inorganic materials surfaces have been improved like Non-covalent enzyme immobilization and Covalent linking of enzyme immobilization.

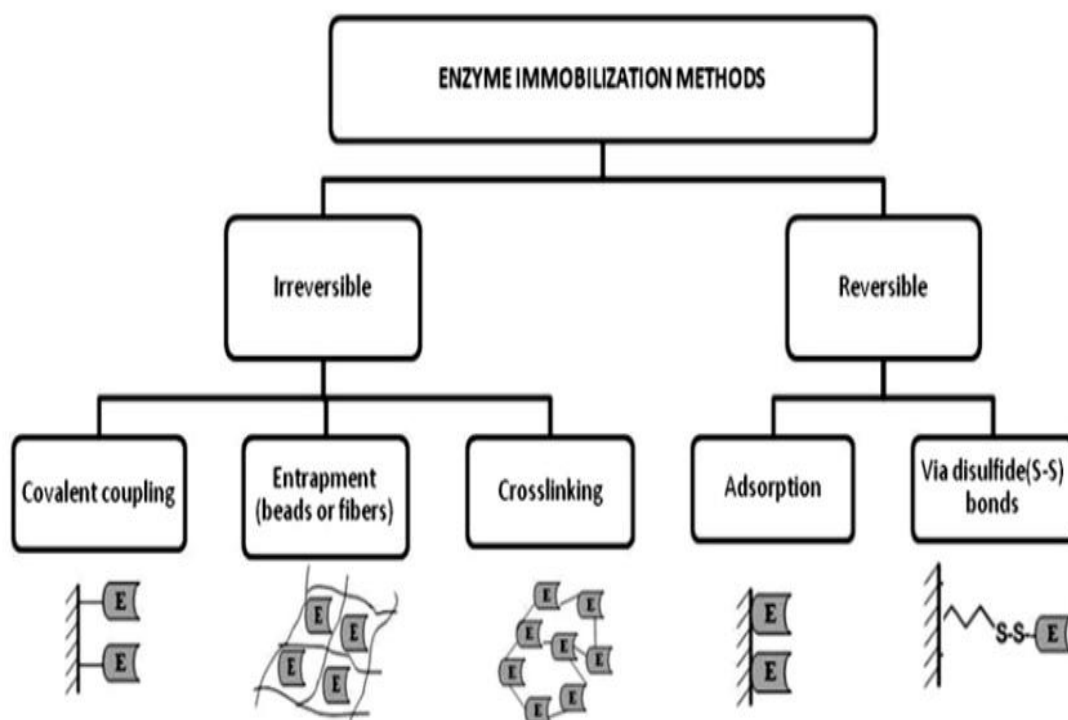


Figure 2.5. Schematic illustration of different type of enzyme immobilization methods [29].

Alcohol biosensor has been fabricated using either alcohol oxidase AOx or alcohol dehydrogenase ADH by enzyme immobilization methods. Glucose biosensor is fabricated by using different type of enzymes for example glucose oxidase (GOx), glucose dehydrogenase (GDH) and isoenzyme 2 of hexokinase (HK) [44].

#### 2.4.1. Non-covalent enzyme immobilization

Non-covalently immobilization of enzymes including different methods such as: Direct physical adsorption: This method is carried out under sonication. However, it is not appropriate for most of enzymes, which are carried out under sonication during the adsorption process as sonication can create high pressure gradients and furthermore influence the protein structure. The method of physical adsorption immobilize enzymes on the CNTs surface is showing in Figure 2.6.

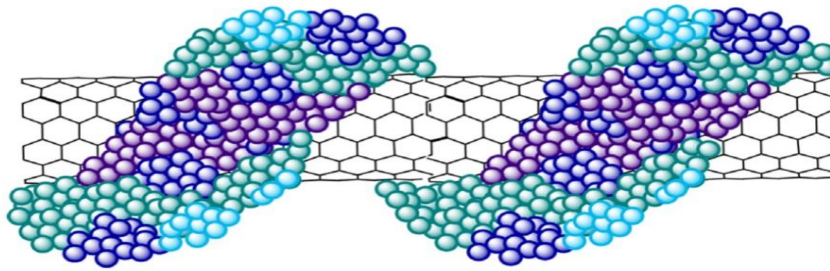


Figure 2.6. Physical absorption of enzyme on CNTs [45]

Enzymes immobilized CNTs modified by polymers: CNTs coated with polymers can supply positively and negatively charged functional groups to CNT modified polymer surface, and for fabricating biosensors, enzymes have been immobilized with the electrostatic interactions onto nanotube composites [46].

Enzymes immobilized CNTs modified by biomolecules: The DNA-based biomolecular detection principle had utilized for CNTs for fabricating carbon nanotubes modified DNA electrochemical biosensors [47].

Enzymes immobilized CNTs modified by with the help of surfactants: Carbon nanotubes are sonicated in the surfactant solution like sodium cholate [48].

Layer-by-layer methods for enzyme adsorption: By enhancing the enzyme layers which are immobilized on the surface of CNTs, the activity of biocatalytics can be greatly increased. Figure 2.7. illustrates LBL deposition technique of GOx on the surface of SWCNTs.

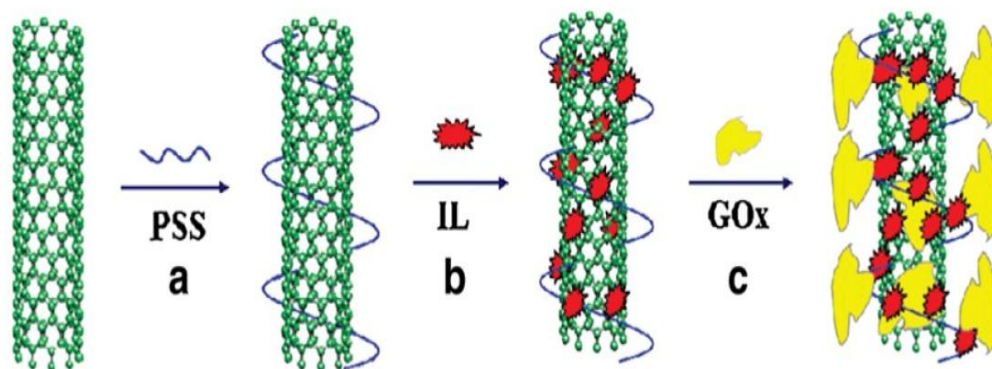


Figure 2.7. Representation of glucose oxidase immobilization on SWNTs surface of by layer-by-layer immobilization technique. PSS: poly (sodium 4-styrenesulfonate); IL: ionic liquid with permission [49]

#### 2.4.2. Covalent Linking

Covalent linking of enzymes onto the surface of CNTs directly: For producing biosensors, enzymes have already been covalently adsorbed onto the surface of carbon nanotubes and demonstrated significant properties higher stability and activity, lower mass transfer resistance and increased reusability as the conjugates always stable under high temperatures.

Covalent linking of enzymes onto the surface of CNTs by adsorbing molecules: The adsorption molecules have great advantages and bring specific sites for immobilizing the enzymes onto the surface of CNTs. The molecules can be linked to the surface of carbon nanotubes by hydrophobic and  $\pi$ - $\pi$  interactions and at the same time covalently linked all enzymes with amide bond [50].

#### 2.5. Glucose Oxidase Immobilization

The detection of glucose concentration has significant role in the fields of biological, clinical, food processing and fermentation and chemical samples. Oxidation of Glucose oxidase can be achieved by using two different techniques. First one is carried out by applying mediators with an indirect method to shuttle that electrons. Mediators which is applied in this sensors contain ferrocene derivatives, quinones and poly-2-aminoaniline polymer. The second one is to fabricate glucose sensor without mediators by directly transferred electrons

between GOx and electrode. However, it is quite difficult to transfer the electrons between the electrode and enzyme, furthermore, immobilizing and stabilizing enzyme process needs inconvenient approach. Thus, the unmediated sensors facing limited sensitivity and application [51].

GOx has considerable application in different fields of area such as canned drinks, ejecting oxygen from Squash, glucose extracting from dried egg and colour improvement, taste and extension application on foods and in wine production.

### **2.5.1. Glucose Oxidase Properties**

GOx is generally purified from the *Aspergillus niger* and *Penicillium amagasakiense*, and for GOx productions, *Aspergillus niger* is the most applied species. Molecular weight of Glucose oxidase is ranged from 130 to 175 kDa. GOx has high specificity to the  $\beta$ -anomer of D-glucose rather than  $\alpha$ -anomer. GOx activity results reduced when applying substrates such as D-galactose, D-mannose and 2-deoxy-D-glucose. Sodium bisulphate, hydrazine, phenylhydrazine, hydroxylamine and ions as  $\text{Hg}^{2+}$ ,  $\text{Ag}^+$ ,  $\text{Cu}^{2+}$  limit the GOx activity. *Penicillium amagasakiense* has high amount of glucose rather than *Aspergillus niger*, while the amount of mannose and hexosamine in *Aspergillus niger* is higher than *Penicillium amagasakiense*. *A. niger* has 16% amount of carbohydrate while *P. amagasakiense* has 11%. The optimal pH range of GOx which is purified from *A. niger* is 3.5-6.5 while it is 4.0-5.5 for the GOx purified from *P. amagasakiense* [52].

### **2.5.2. Glucose Oxidase Reaction Mechanism**

GOx catalysis the oxidation of  $\beta$ -D-glucose to D- gluconolactone and hydrogen peroxide and during the reaction  $\text{H}_2\text{O}_2$  is applied as an electron receiver. The oxidation reaction can be carried out by two steps such as oxidative and reductive step.  $\beta$ -D-glucose is oxidized to D- gluconolactone during the reductive half-reaction, and the D- gluconolactone is hydrolyzed to gluconic acid without using enzyme. Subsequently, FAD (flavine adenine dinucleotide) which is the prosthetic group of GOx is reduced to  $\text{FADH}_2$ . However, during the oxidative half-reaction, the reduced GOx is being oxidized again by molecular oxygen to yield  $\text{H}_2\text{O}_2$  [53]. Figure 2.8 illustrates the GOx catalysis reaction.

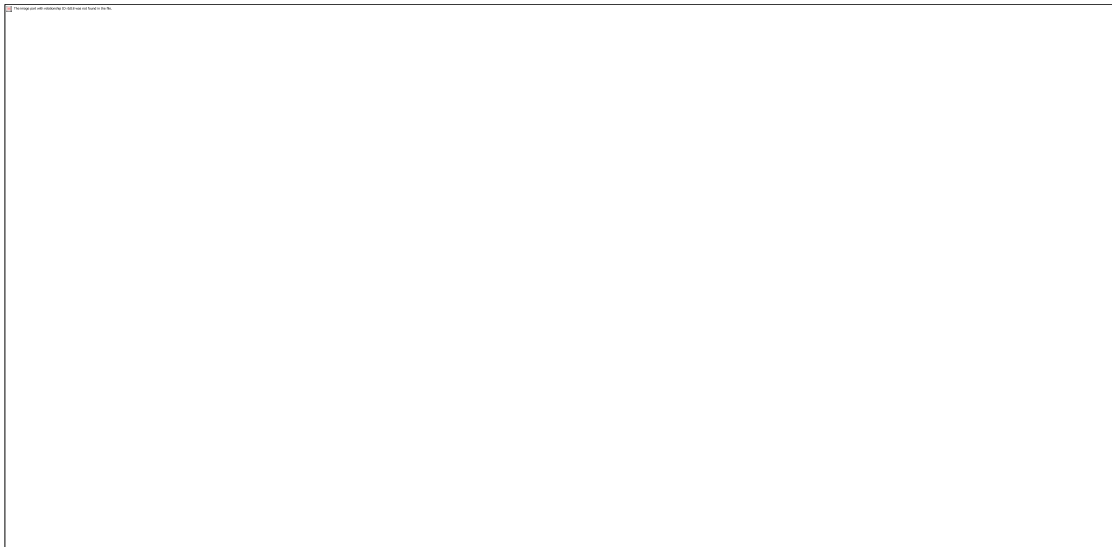


Figure 2.8. Illustration of Glucose oxidase catalysis reaction [53]

Two different reaction mechanisms have been suggested for reductive half-reaction such as hydride separation and nucleophilic attack after deprotonation (Figure 2.9).

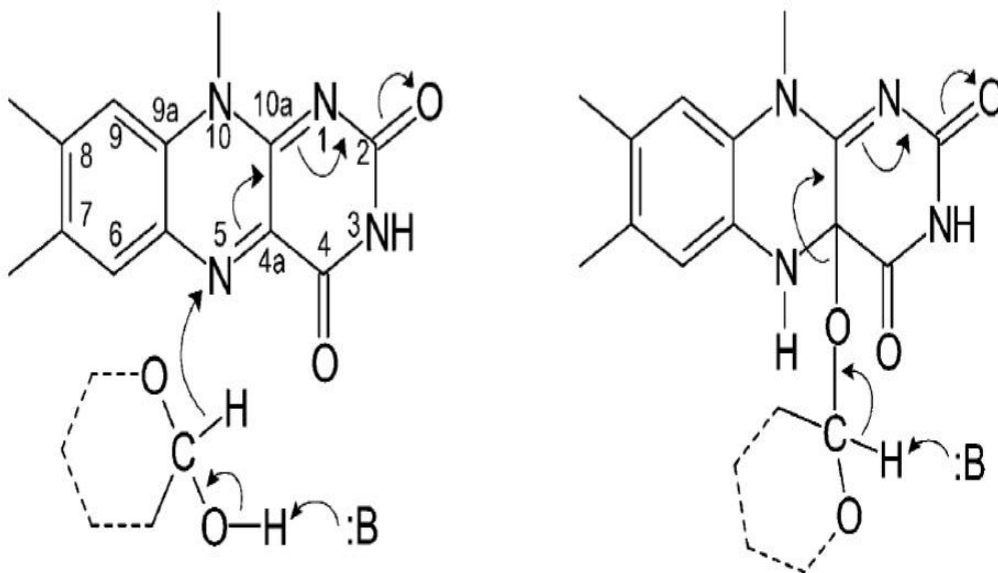


Figure 2.9. Schematic illustration of two different mechanisms proposed for reductive half-reaction [53].

### 2.5.3. Glucose Oxidase Activity Analysis

For accurately detecting the activity of GOx, two different methods are widely being applied by researchers. The first one is the titrimetric method, and the next one is based on colour change analysis which is named analytical method.

Tongbue et al. (1996) applied titrimetric method for the detection of GOx activity. GOx solution was injected into the sodium acetate buffer solution which includes 2% of  $\beta$ -D-glucose, then sodium hydroxide solution was added. To measure the hydrochloric acid added volume, the final solution was then titrated with hydrochloric acid for detecting the activity of GOx [54].

In analytical method,  $H_2O_2$  which is achieved through the oxidation of  $\beta$ -D-glucose by molecular oxygen is applied to oxidase a chromogenic substrate with the existence of horseradish peroxidase (HRP) and the colour change is occurred. Chromogenic substrate means generally a colourless chemical which is used to add colour to the enzymes being tested and hereby to define enzyme activity. Chromogenic substrate includes 2,2'-Azino-di-[3-ethylbenzthiazolin-sulfonate] (ABTS) and o-dianisidine. ABTS forms green-blue product that is examined by spectrophotometers at 420 nm while the oxidation of o-dianisidine is measured with spectrophotometers at 500 nm. Figure 2.10. represents the GOx reaction with ABTS [55].

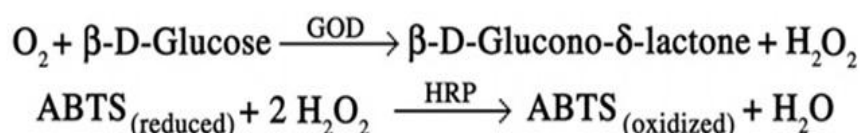


Figure 2.10. Schematic illustration of GOx reaction with ABTS [55].

For the detection of GOx activity with chromogenic substrate of o-dianisidine, several studies were carried out with benzoquinone, which is based on the reduction of benzoquinone by hydroquinone. During the measurement with spectrophotometer, absorbance rate enhanced at 290 nm. Figure 2.11. representing the reaction between GOx and chromagenic dye o-dianisidine [56].



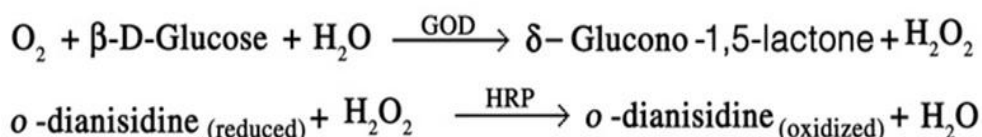


Figure 2.11. Schematic illustration of GOx reaction with chromagenic dye o-dianisidine [56].

## 2.6. Alcohol Oxidase Immobilization

Alcohol oxidase demonstrate characteristic absorption spectra of flavoproteins, which is purified from *H. polymorpha*, *P. pastoris* and *Torulopsis*. AOx may categorized into four different groups based on the specificity of the substrate such as AOx with short chain and AOx with long chain, secondary alcohol oxidase and aromatic alcohol oxidase. It has been studied on the researches that all enzymes have a flavin adenine dinucleotide (FAD) prosthetic group, which is linked to each subunit and has significant influence on molecular activity. The molecule loses activity when FAD is changed or stripped from the subunits. However, one of the main problem is that AOx has limitation on shelf life and processing stability. Consequently, it is necessary to develop adsorbing platforms for enhancing the storage and operational stability. Detection and qualification of alcohol concentration with the application of enzymes becomes an favorable method due to high sensitivity, specificity and activity under very mild operational condition.

For determination of ethanol and other aliphatic alcohols such as methanol, several analytical methods have been researched including colorimetric methods, redox titrations, refractive index and specific gravity analysis, spectroscopic and chromatographic methods. However, these techniques are quite time consuming and at the same time needs distillation and complex process as well as more expensive instruments. All of these disadvantages can be get over by using enzyme immobilization methods [57].

### 2.6.1. Properties and Application of Alcohol Oxidase

Alcohol oxidase is formed of short-chain, linear aliphatic alcohols and oxidizes ethanol and methanol. AOx is formed of eight different subunits, and each of the subunits have one bound azide molecule. The inhibitors include azide,  $\text{Cu}^{++}$ ,  $\text{Ag}^+$ ,

Hg<sup>++</sup>, p-chloromercuribenzoate, hydroxylamine and NaF. The ideal range of temperature is 40-45 °C and the enzyme solubility conversely related to temperature, furthermore freezing does not influence the enzyme activation. The ideal pH range of Alcohol oxidase is in 7.5-8.0 and, refrigeration is inversely related to solution cloudiness in which the precipitation is formed. The enzyme can be solved in phosphate buffer greater than 0.1 M under the pH condition of over 7.0 and the molecular weight of the enzyme is about 630,000. These boundaries for AOx can be enlarged under specific temperature, pH, and ionic conditions.

Applications: AOx biosensors has significant application in different fields of food technology, clinical chemistry, blood, serum, and urine analysis, fermentation, oxygen scavenging, alcohol removal, as well as qualitative or quantitative determination of methanol or ethanol etc [58].

### **2.6.2. Alcohol Oxidase Reaction Mechanism**

For determination of alcohol, two different enzymes have been mostly used such as alcohol oxidase (AOx) and alcohol dehydrogenase (ADH). Alcohol dehydrogenase catalyses the reversible oxidation of aromatic and primary aliphatic alcohols except methanol. However, ethanol biosensors based on ADH is more specific and stable rather than that biosensors based on AOx. Alcohol oxidase is the first enzyme which is able to oxidase both ethanol, methanol, propanol and butanol. AOx is an efficient catalyst for oxidizing lower primary alcohols to the corresponding aldehydes by the mechanism with two-step: the first one is the reductive half-reaction, in which the substrate can be oxidized while FAD is reduced to FADH<sub>2</sub>. Second is an oxidative half-reaction, in which the flavin oxidized again by O<sub>2</sub> and H<sub>2</sub>O<sub>2</sub> is produced.

Alcohol oxidase is thus catalyzing irreversible oxidation of alcohols with lower molecular weight with O<sub>2</sub> as the electron acceptor to the corresponding aldehydes with the concomitant release of H<sub>2</sub>O<sub>2</sub>. Figure 2.12. represents the AOx catalyzes reaction.

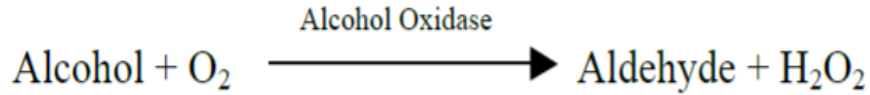


Figure 2.12. Schematic representation of Alcohol oxidase catalyzes reaction [58].

The oxidation reaction can be carried out by using the two enzymes, named alcohol dehydrogenase (ADH) and alcohol oxidase (AOx). AOx catalyzes the oxidation of alcohols into corresponding aldehydes, however the reversed reaction is different from that catalyzed by ADH (Figure 2.13. a). ADH requires NAD-based cofactors when AOx needs flavin-based factors. The FAD transfer the hydride ion to molecular oxygen and hereby form the H<sub>2</sub>O<sub>2</sub> (Figure 2.13. b).

The NAD<sup>+</sup> (or NADP<sup>+</sup>) receive the hydride ions from that substrates during the catalysis reaction and form NADH [59].

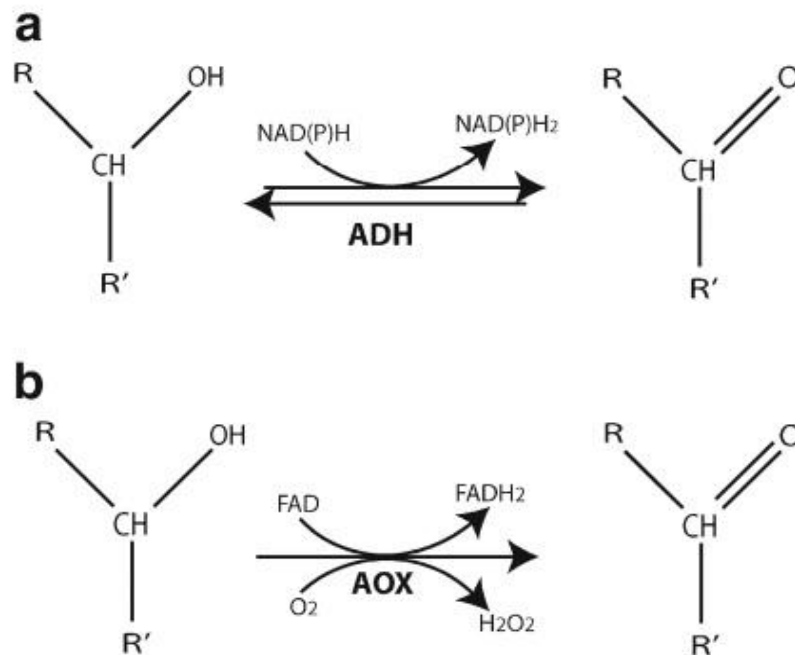


Figure 2.13. Schematic representation of a) Alcohol dehydrogenase (ADH) as catalyst, b) alcohol oxidase (AOX) as catalyst [59].

### 2.6.3. Alcohol Oxidase Activity Analysis

Activity of alcohol oxidase having been measured with oxidase-catalysed reaction by the increase of  $H_2O_2$  concentration or the decrease of  $O_2$  tension.

AOX Activities was firstly studied in 1960. in a *Polystictus versicolor* culture. Alcohol oxidase activity can be measured by two different methods which is carried out by examining the increment of  $H_2O_2$  in the mixture or by measuring the decrease of  $O_2$  tension which is involved in the catalytic reaction of AOx by using optical or electrochemical detections.

The concentration of  $H_2O_2$  is measured by using horseradish peroxidase (HRP), which oxidizes chromogenic substrates during  $H_2O_2$  reduction reaction (Figure 2.13), and generate the colour change. The chromogenic substrates including 2,2'-Azino-di-[3-ethylbenzthiazolin-sulfonate] (ABTS) and o-dianisidine. ABTS forms bluish green colour product that is examined at 415 nm while the oxidation of o-dianisidine is measured with spectrophotometers at 530 nm. The oxygen-based detection has some limitations due to the high background signal and hereby lower sensing ratio of substrate alcohol as well as low accuracy and reproducibility. However,  $H_2O_2$  based sensors demonstrate significant properties such as manufacturing easily and at the same time fabricating the sensors in small sizes.

For the detection of free alcohol oxidase activity, alcohol solutions were prepared immediately before use in a phosphate buffer (pH 7.5) and the alcohol solution was placed in test tubes in water bath at a specific temperature condition. Enzyme and substrate reaction were carried out by adding the enzyme solution to alcohol, then peroxidase (POD) was added to catalyze the reduction of  $H_2O_2$  and hereby oxidation of o-dianisidine. Finally, after adding sulfuric acid, the reaction was stopped. The oxidation of o-dianisidine is measured with spectrophotometers at 530 nm.

For enzyme electrodes, the same procedure was used by adding the enzyme electrode into the alcohol solutions instead of adding free enzyme. Figure 2.14. shows the schematic representation of alcohol oxidase reaction with chromagenic dye o- dianisidine and ABTS respectively [60].

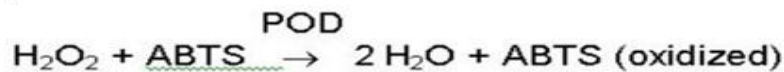
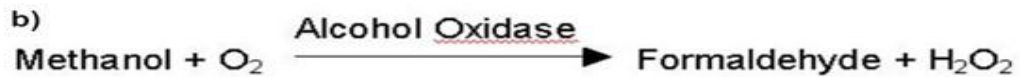
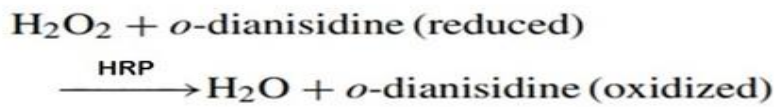


Figure 2.14. Schematic representation of a) Alcohol oxidase (AOD) reaction with chromagenic dye o- dianisidine, and b) Alcohol oxidase reaction with ABTS

## 2.7. Polyvinyl Alcohol (PVA)

Poly (vinyl alcohol) is a synthetic polymer that has been used to immobilize various biological cells and enzymes for 30 years. Several researches have already been focused on application of PVA (Poly (vinyl alcohol)) on enzyme adsorption for the process of electrospinning as a material because of its significant characteristics in forming fibers and membrans. PVA is hydrophilic and can be functionalized easily by the hydroxylic group. For immobilization, to generate membrane or hydrogels, PVA is applied in different cross-linked forms. PVA is produced through polymerizing the vinyl acetate to polyvinyl acetate (PVAc) and hydrolysis of polyvinyl acetate to remove the acetate groups (Figure 2.15).

PVA is produced by three different methods such as aminolysis, alkaline hydrolysis and acidolysis. During the alkaline alcoholysis method which is used in the industrial process, the acetate groups are hydrolyzed by methanol interchanged ester with sodium hydroxide and hereby convert PVAc to PVA [61].

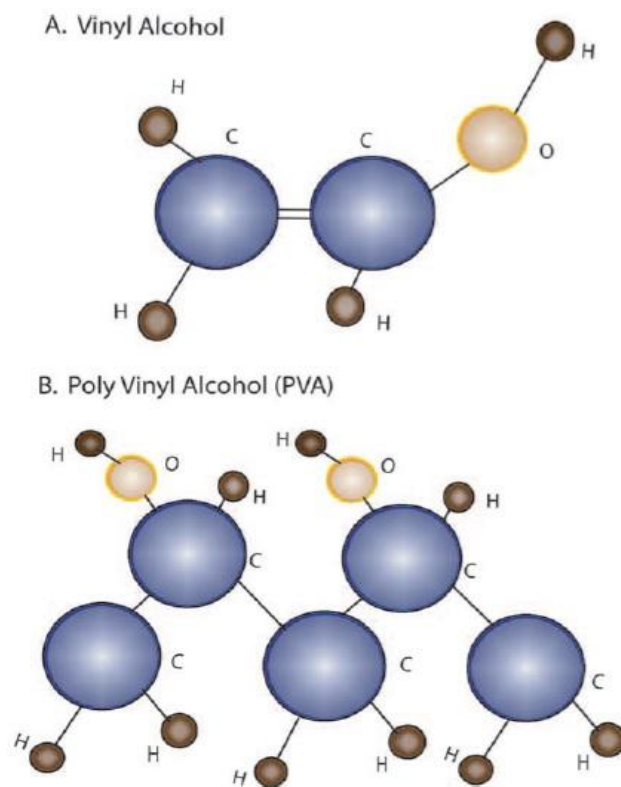


Figure 2.15. The illustration of chemical structure of PVA and vinyl alcohol B: PVA is synthesized [61].

### 2.7.1. Properties and Application of PVA

PVA has unique mechanical, chemical and physical properties. It is in the class of non-ionic, water soluble and nonhazardous polymers that also showing low protein adsorption and biocompatible characteristics. PVA generally available in powder form and it is the tasteless, odorless and diaphanous polymers which has low environmental impact, and the physical properties can be influenced by the amount of hydroxylation. Higher degree of hydroxylation and polymerization of PVA resulted in enhanced water resistance and enhanced adhesive to the surface of hydrophilic. Decreased amount of hydrolysis can be influenced in decreased water solubility, increased flexibility, and increased difficulties to crystallize.

The rubber elastic physical properties of PVA and the tensile strength of hydrogels results different field of application fields including artificial cartilage replacement. Besides, PVA hydrogels having been applied in the area of biomedical like

artificial pancreas synthetic vitreous humor, contact lenses, hemodialysis, and meniscus tissue [62]. Polyvinyl alcohol also applied in medical areas including artificial tears, vascular embolism treatment, and neurologic regeneration, as well as tissue adhesion barriers. Additionally, Polyvinyl alcohol is also widely applied in the area of textile industries such as producing paper products, and in food packaging systems as PVA films demonstrate significant barrier properties. Due to its nontoxic, noncarcinogenic and swelling properties, PVA having been commonly used in the area of medical devices [63].

### **2.7.2. Cross-linking of PVA**

Cross-linking is an important method for the modifying the existing polymers to get an improved material. PVA needs to be cross-linked for generating hydrogels because of its water solubility. As it has been indicated from the researches, cross-linked PVA has great stability in high acidic or in high alkaline medium. Being a biodegradable synthetic polymer, PVA hydrogels has been researched to incorporate bio-active materials due to its similarity to living tissue. For instance, a preventing mechanism for the overdosing and rejection problems can be carried out by modifying the water swelling degree and hydrophilicity of PVA and hereby, to control the drug delivery quotient in human body. Besides, for studying the cells or biomolecules functions in non-living media, molecules or cells can be immobilized in this life-mimicking systems. The cross-links provide structural stability and the degree of cross-linking determines the physical, diffusional and chemical properties of PVA.

Non-crosslinked PVA structure is not stable in water, and the integrity structure can be damaged by aquatic medium to influence its performance. Techniques for cross-linking of PVA are based on the physical, chemical and heat treatment, and cross-linking provides resistant supporting network for immobilization of cells or molecules. During the heat treatment process, heat energy is used to modify the spatial organization of chains and to assemble stronger hydrogen bonds from hydroxyl groups [64]. In physical technique, increasing degree of crystallinity results a decrease in the water content of polymer, therefore, this method is not stable as other methods. Chemical cross-linking can be carried out by the reaction between the hydroxyl group and cross-linker. All multifunctional compounds which is able to react with the hydroxyl group can be applied as a cross-linker for PVA.

Different cross-linking agents such as dialdehydes, dicarboxylic acids, dianhydrides have already been used for PVA functionalization. Among them, Polyvinyl alcohol which is cross-linked with Dicarboxylic acid is mostly preferred by researches. In the present work, glutaraldehyde (GA) is the most applied cross-linking agent due to nonspecifically binding property of GA as proteins by its two active sites, which can bind both protein and PVA. In this procedure, the film is immersed into the alcoholic solution contains the mineral acid and cross-linking agent, like HCl or H<sub>2</sub>SO<sub>4</sub>. The alcoholic medium is applied to swell the membrane to diffuse the protonic ions and dialdehyde molecules. Figure 2.16. shows the mechanism for the reaction during cross-linking between the GA solution and PVA electrospun fibers [65].

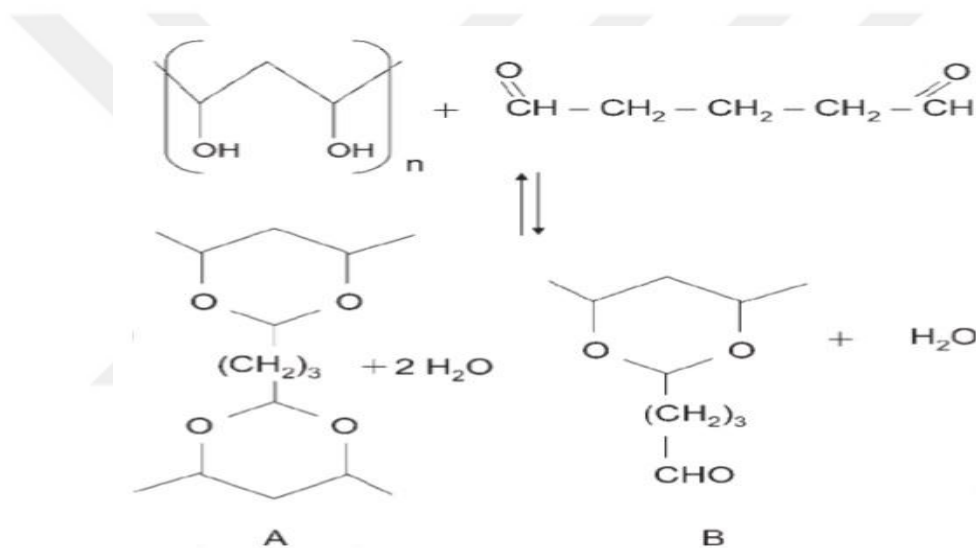


Figure 2.16. Mechanism of cross-linking reaction between PVA and GA [65].

## 2.8. Scanning Electrochemical Microscopy (SECM) Analysis

The scanning electrochemical microscope (SECM) is used for detecting the electron-transfer reaction of tip generated species which occurred on the surface of nonconductive and redox-active enzyme containing surfaces. This technique applies an ultra-micro electrode (UME) probe which is immersed in a solution near to the sample surface. Mass transfer between electrode-interface and chemical reaction determine the response of the electrode that occurred on the surface of the sample. furthermore, when the tip is at the large distance from the surface of



the sample, usually a distance more than 10 UME radii, the response of the UME is the steady state current under semi-infinite diffusion conditions which depends upon only the characteristics of the electrode itself and the mediator (Figure 2.17. a). While the distance between sample surface and injector tip is decreased, UME current changes due to the interaction between diffusion layer and sample. If the surface is insulator or the substrate is nonreactive, UME current decreases when it is approaching to the sample because the surface blocks the diffusion of the reacting species and hereby produce a negative feedback (Figure 2.17.b). The surface intercepts the applied mediator species which is formed on the tip and reformed R for conductive surfaces when the probe-sample distance is small. (Figure 2.17.c) [66].

Applications of SECM containing fabrication in micro-scale and imaging at a liquid-solid interface, probing the kinetics of solution reaction at the surface of conductive substrate [67].

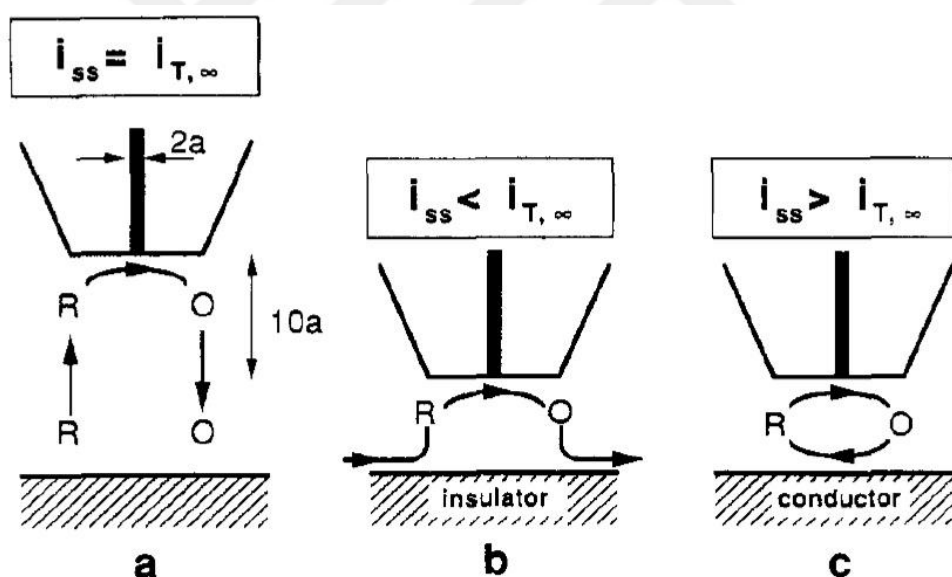


Figure 2.17. Scanning electrochemical microscopy working principle. (a) By using the UME far, (b) Diffusion on an Insulating substrate, (c) Diffusion on a conductor, and the mediators are generated again [66].

### 3. EXPERIMENTAL SECTION

#### 3.1. Materials

Polyvinyl alcohol (PVA, 87-90% hydrolyzed,  $M_w = 30-70 \text{ kg mol}^{-1}$ ) were purchased from Sigma-Aldrich, D(+)-Glucose (99%) were purchased from AppliChem, glucose oxidase (GOx, EC 1.1.3.4 *Aspergillus niger*, 50 KU, Sigma), Poly(diallyldimethylammonium) chloride solution (PDDA,  $M_w=400000-500000$ ) were purchased from Sigma-Aldrich, MWCNTs (9-10 nm in diameter, NC700<sup>TM</sup>) and SWCNTs (2 nm in diameter, NC110<sup>TM</sup>) were purchased from Nanocyl, Glutaraldehyde (25%, Alfa Aesar), Nitric acid ( $\text{HNO}_3$ , 65%, Merck) and Sulfuric acid ( $\text{H}_2\text{SO}_4$ , 95.0-98.0%, Sigma-Aldrich) were used for the purification and functionalization of CNTs, Ethyl Alcohol (99.5%, Tekkim), Acetone (99.5% Honeywell), Phosphate Buffer Salin (PBS, Sigma) were applied for preparing glucose and glucose oxidase aqueous solution, Pencil graphite (0.9 mm in diameter, Tombow) was applied for producing sensor electrode, Potassium hexacyanoferrate (III) trihydrate ( $\text{K}_3\text{Fe}(\text{CN})_6 \cdot 3\text{H}_2\text{O}$ , 98.5-102.0%, Sigma Aldrich) and Potassium chloride (KCl, Sigma-Aldrich) were applied during the GOx electrochemical measurements. All other chemicals were of analytical grade, and all the aqueous solutions were prepared using doubly distilled water.

#### 3.2. Methods

By manipulating the structural design and composition of nanocomposite membranes, glucose sensing efficiency of five different sensor electrodes a) *Glucose oxidase (GOx) immobilized PVA electrospun electrode*, b) *Glucose oxidase (GOx) immobilized PVA electrospun electrode functionalized with multi-walled carbon nanotube (MWCNT)*, c) *Glucose oxidase (GOx) immobilized PVA electrospun electrode functionalized with PDDA modified multi-walled carbon nanotube (MWCNT)*, d) *Glucose oxidase (GOx) immobilized PVA electrospun electrode functionalized with PDDA modified single-walled carbon nanotube (SWCNT)*, e) *Glucose oxidase (GOx) immobilized, and Interfacially cross-linked PVA electrospun electrode functionalized with PDDA modified multi-walled carbon nanotube (MWCNT)* were comparatively studied.

### **3.3. Pretreatment of SWCNTs and MWCNTs**

SWCNTs and MWCNTs should be purified and functionalized before applying in the CNT modified PVA section. For the preparation of purified carbon nanotubes, 0.5 g of each CNT type were sonicated in the aqueous solution of HCl (100 mL, 1.3 M) for 48 h at 70°C respectively. After that, nanotube suspension of each CNT type were diluted with using double distilled water until the pH of the solution was reached to 7.0, and thereafter filtered with a 0.22 µm pore sized cellulose acetate membrane. Finally, the residue was dried at 50°C under vacuum nearly for 1 h.

For the preparation of shortened and oxidized SWCNTs and MWCNTs, 0.4 g of each purified CNT type were sonicated in 36 ml of concentrated nitric acid (70%, Sigma Aldrich) and concentrated sulfuric acid (95.0–98.0%, Sigma Aldrich) in 1:3 volumetric ratios for 2 h (for SWCNTs) and 4 h (for MWCNTs), at room temperature. After that, the achieved solution was treated by ammonium hydroxide till the pH of the prepared solution was reached to natural, after that filtered with a 0.22 µm pore sized cellulose acetate membrane. Finally, to remove the salt residues, filtered CNTs were washed with double-distilled water and dried at 70 °C for 1 h in oven.

### **3.4. Preparation of CNTs Modified PVA Nanofiber Membrane**

Firstly, we prepared a homogeneous solution of neat PVA nanofiber membrane. For this, 10 g of PVA powder was prepared and thereafter added into 100 ml of distilled water. The prepared mixture was heated and stirred at 75 °C for 4 h, after that, the prepared solution was kept at room temperature to prepare 10 % ( wt) of PVA homogeneous solution.

For producing CNTs modified PVA nanofiber membrane, purified and functionalized CNTs added into the PVA solution (10%). Mass ratio of PVA: CNT was fixed to 100:4. After this, the mixture solution was stirred at room temperature for 24 h to prepare a homogenous solution of CNTs modified PVA nanofiber membrane.

During the electrospinning process, we placed the polymer solution in a 20 ml plastic syringe has steel needle which was connected to the high voltage supply with a 28 kV of potential difference. The distance between the needle and the collector was adjusted as 25 cm. By applying the micro syringe pump, flow rate

was set as 4 ml/h. The mat like PVA fibers were then deposited on the surface of grounded aluminum collector. After dried at room temperature for 24 h, the mat like PVA fibers were detached from the surface of the collector. Scanning Electron Microscope was applied to observe the morphologies of electrospun membranes (FEI QUANTA250 FEG, Oregon, USA). After then, the fibers were selected randomly from each of the SEM micrographs, and each fiber diameter was obtained by using Image-J software.

#### **3.4.1. PVA Coating of Pencil Graphite Electrode**

Two different methods for coating the surface of pencil graphite electrode with PVA electrospun nanofiber can be carried out for getting a homogenous fiber mat thickness such as, home-made rotating system and stable coating system. In the process of home-made rotating system, pencil graphite electrode is fixed on a styrofoam which has 1 mm thickness and 2 cm diameter size. Thereafter it is placed on a beaker (50 ml) which has water up to half of it, and the beaker is situated between the injector tip and the collector. During the process, the pencil graphite electrode can be rotated upon itself by the circulation of water with magnetic stirrer. Figure 3.1 shows the typical electrospinning setup in our laboratory.

In the stable coating method, what is different from the previous coating system is that there is neither rotation nor collector in the coating process. We used stable coating method during our process, and firstly pencil graphite electrode was fixed onto the drum collector under a stable condition from its edge surface, and the process of fiber coating was carried out (Figure 3.2). Inovenso Ne 300 electrospinning device was used during this process.

For controlling the thickness of PVA fiber mat on the surface of graphite electrode, three different spinning time was processed under room temperature: 1, 2, and 5 min. The fixed potential difference was 28 kV, flow rate was fixed as 4 ml/h, and the distance between tip to pencil graphite electrode was fixed as 25 cm, and the fiber thickness on the surface of pencil graphite electrode was obtained by using SEM.



Figure 3.1. Typical electrospinning set up in our laboratory

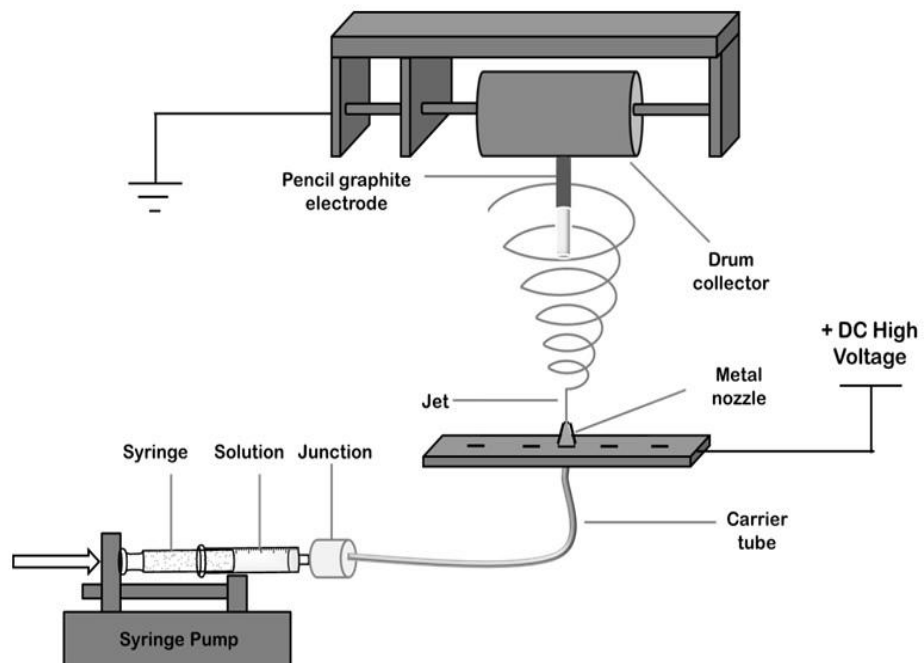


Figure 3.2. Schematic illustration of pencil graphite electrode fiber coating set up with stable coating system [68]

### **3.5. Preparation of Cross-linking PVA Electrospun Membranes**

PVA electrospun membrane cross-linking process was carried out by using GA (Aldrich, aqueous solution, 50 wt %). Firstly, we prepared 226  $\mu\text{l}$  GA and 25  $\mu\text{l}$  HCl containing 5.749 ml acetone solution in a beaker in the order of firstly acetone, then HCl and finally GA. After that, the CNT modified PVA electrospun membranes were immersed in cross-linking GA solution. For investigating the influence of cross linking time on the morphology of electrospun nanofibers and for obtaining the optimal cross-linking time data, 1, 3, and 24 h cross-linking results were observed.

After preparing Cross-linked PVA electrospun membranes, the membranes were washed with ethyl alcohol and PBS buffer (pH 7.0) respectively after removing from the solution. After that, we dried the membranes for 20 h under room temperature, and the morphology of these membranes before and after cross-linking were studied by using SEM. For the investigation of fiber diameter distribution, we used ImageJ software and obtained all the data by statistical analysis of SEM micrographs. Before and after cross-linking of the membranes, FTIR-ATR tests were carried out for characterizing the membrane properties such as cross-linking density and chemical structures.

### **3.6. Interfacial Cross-linking of PVA Nanofiber Mat**

For fabricating interfacially cross-linked PVA electrospun nanofibers, 150 mg of oxidized MWCNT was added into 75 ml of GA solution. After that, it was sonicated for 50 min at room temperature, and then neat PVA electrospun nanofiber coated pencil graphite electrode was immersed into that cross-linking solution and kept for 1 h. At the end, the graphite electrode was washed firstly with ethanol and then with PBS (pH 7), and kept at room temperature for 3 h to be dried. Consequently, interfacially cross-linked, and CNTs modified PVA electrospun membranes were obtained.

### **3.7. Preparation of CNT- (PDDA/GOx)<sub>2</sub> Conjugate**

After fabricating functionalized CNT modified PVA fiber structure, 10 wt % PDDA aqueous solution was sonicated for 1 h. During this time, we prepared two different enzyme solutions of GOx and AOX immediately before use. The GOx solution containing 2560 unit/ml GOx in 0.1M PBS (pH 7.0), and the AOX solution

containing 0.1 unit/ml AOx in 100 mM cold PBS (pH 7.5). For immobilizing positive charged PDDA on functionalized CNT, we put the pencil graphite electrode in 6 ml PDDA solution and keep it on an orbital shaker +4°C for 17 min, and then the graphite electrode was washed with PBS for removing free PDDA (the washing procedure was repeated at least three times in order to ensure removal of the free PDDA from solution. After this step, for immobilizing negative charged GOx/AOx on functionalized CNT, PDDA immobilized pencil graphite electrode was immersed in 6 ml of GOx solution, and was kept on an orbital shaker +4°C for 20 min, after that, pencil graphite electrode was immersed in 6 ml of AOx solution and was also kept on an orbital shaker +4°C for 20 min. In this process, we obtained two layers of PDDA/GOx/AOx conjugate (Figure 3.3) by repeating the same procedure two times. Finally, pencil graphite electrode which is immersed in GOx/AOx solutions respectively, was incubated at +4°C for 24 h.

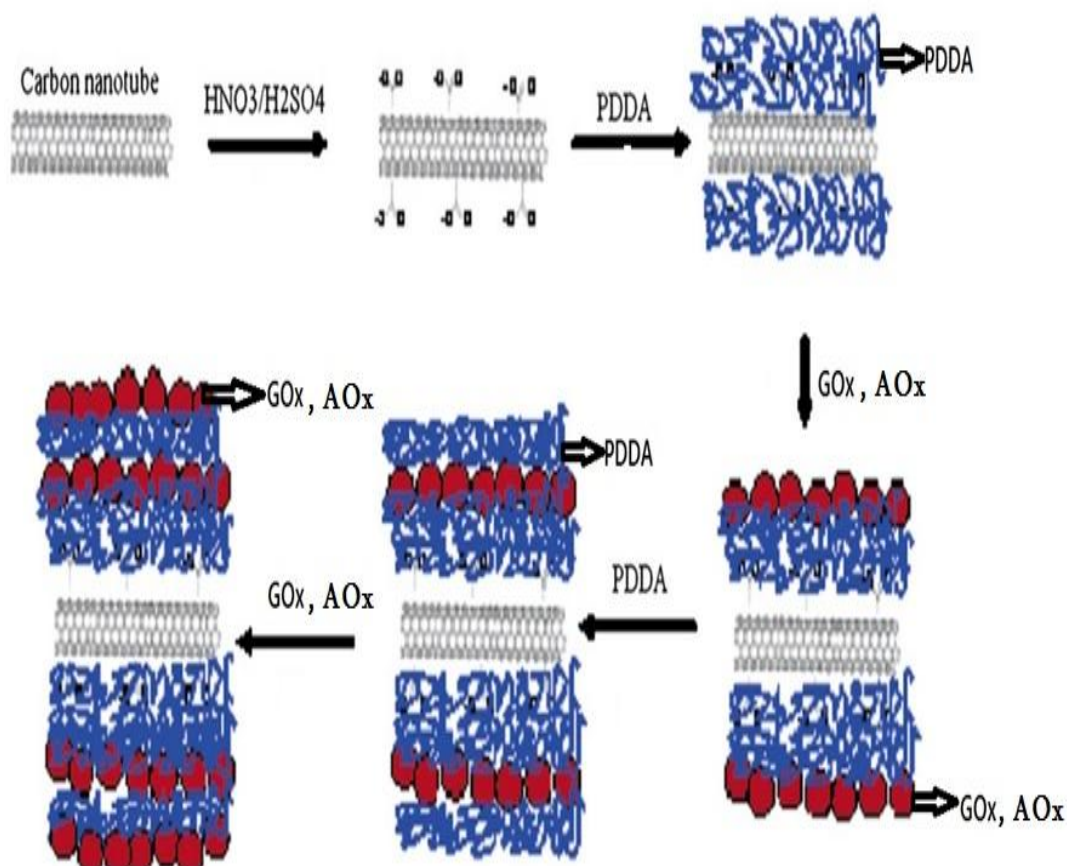


Figure 3.3. Schematic representation of CNT-(PDDA/GOx/AOx)<sub>2</sub> conjugate preparation steps [49].

### 3.8. Electrochemical measurements

#### 3.8.1. Electrochemical measurements of GOx.

In our study, electrochemical measurements of ethanol, methanol and glucose were carried out by using three-electrode electrochemical system (Figure 3.4) containing pencil graphite electrode (PGE) as a working electrode, Pt wire as a auxiliary electrode, and Ag/AgCl electrode as a reference electrode, and Gamry Echem Analyst software was applied during analyzing all the data. Chronoamperometric measurements were carried out under -0.5 V in stirred 0.1 M PBS. Cyclic Voltammetry and Chronoamperometry experiments was carried out using Gamry Instrument Reference 600-Potentiostat/ Galvanostat/ZRA for checking the reproducibility and operational stability of the electrodes, and Cyclic Voltammetry measurements were carried out at a scan rate of  $100 \text{ mV s}^{-1}$  and in an air saturated solutions of  $50 \text{ mM Fe(CN)}_6^{3-}/\text{Fe(CN)}_6^{4-}$  redox couple in 1 M KCl. i-t curve method was applied to detect glucose in PBS, and detecting different concentration of glucose process was carried out by injecting 15 mM glucose solution with varying volumes into stirred PBS.

Electrochemical impedance Spectroscopy (EIS) experiments were carried out applying the AUTOLAB PGSTAT204 Compact and modular potentiostat/Galvanostat, and during the EIS measurements, which were performed in faraday cage, a +0.23 V DC Voltage versus Ag/AgCl and 10 mV of AC signal was used. All the data were achieved under the frequency range of  $10^{-1}$ - $10^5$  Hz. and in a mixture of 25 mM (1:1)  $\text{Fe(CN)}_6^{3-}/\text{Fe(CN)}_6^{4-}$  and 1 M KCl solution.



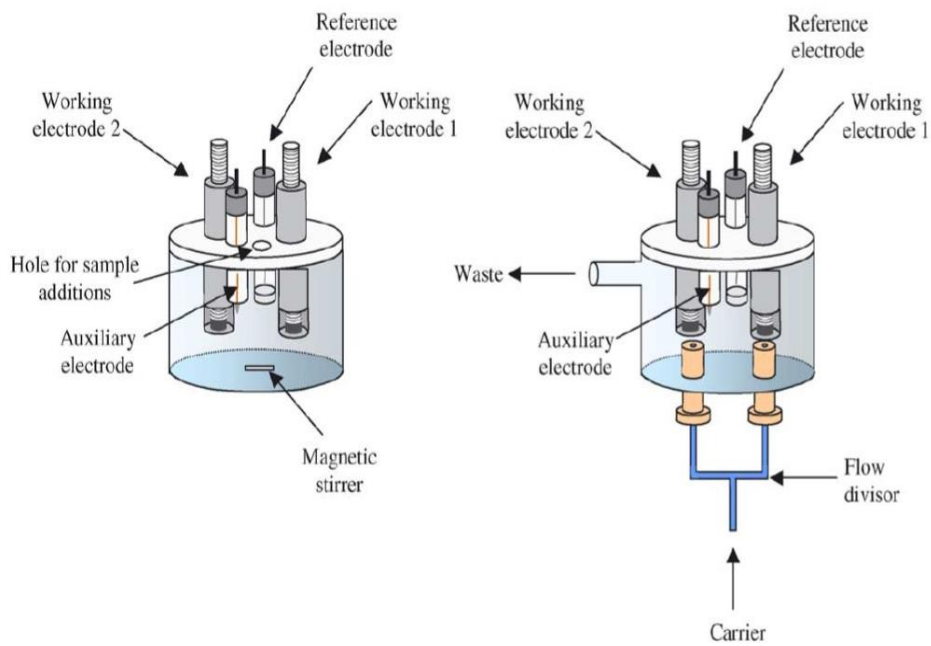


Figure 3.4. Schematic representation of batch and flow-injection cells used for dual amperometric measurements [67].

## 4. RESULTS AND DISCUSSION

### 4.1. PVA Electrospun Nanofibers Characterization

For fabricating sensitive electrospun mat to detect the concentration of ethanol, methanol and glucose, three different processing variables were studied such as applied voltage, solution flow rate and tip-collector distance. During the process, applied voltage was fixed at 28 kV, flow rate was monitored as 4 mL/h and the distance between tip and collector was fixed at 25 cm. The average electrospun PVA fibers diameter was measured as 100 nm. The spinning solution concentration was fixed at 10 wt % and hereby continuous and smooth formation of fibers was achieved (Figure 4.1.a). Photographic image of neat PVA electrospun nanofibers is shown in figure 4.1.b). After cross linking, the smooth and continuous morphology of nanofibers was not obviously changed while the average fiber diameter was enhanced (Figure 4.1.c). Due to the swelling of nanofibers during the cross linking process, average fiber diameter resulted in increased. Three different spinning time was processed: 1, 3, and 24 h. Figure 4.1. represents the SEM image of neat PVA electrospun nanofibers and its fiber diameter distributions. Figure 4.2 shows SEM micrograph of PVA electrospun membranes under different cross-linking time and the fiber diameter distribution. For 1 h cross linking, the the electrospun nanofibers average fiber diameter was measured as 117 nm and after 3 h cross linking, the electrospun nanofibers average fiber diameter was reached to 122 nm while this value is increased to 160 nm after cross linking for 24 hours.

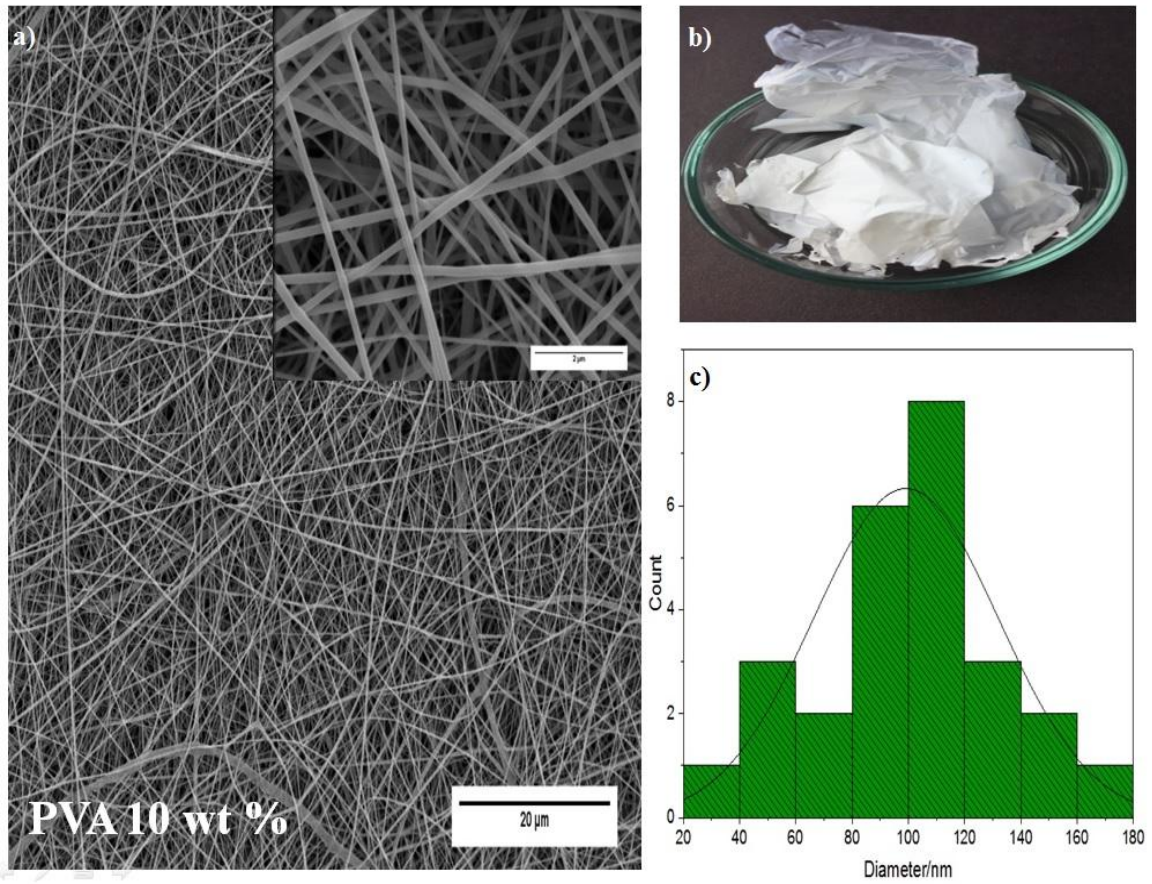


Figure 4.1. a) SEM image of 10 wt% PVA, b) Photographic image of PVA nanofibers, c) PVA electrospun nanofibers fiber diameter distribution.

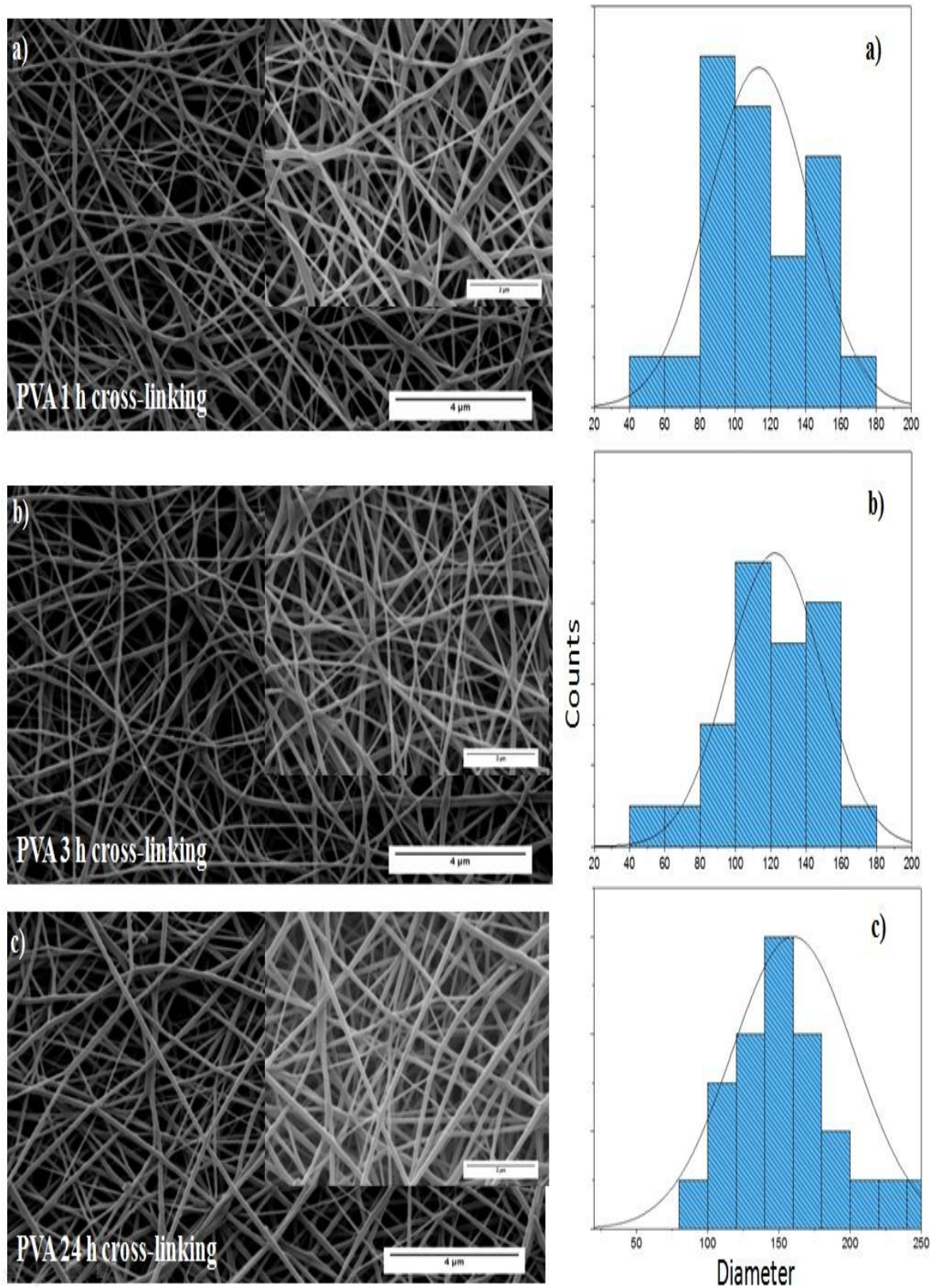


Figure 4.2. SEM image cross-linked PVA nanofibers and the fiber diameter distribution a) 1h, b) 3h, c) 24 h

Table 4.1. Characteristics of before and after cross linking of PVA nanofibers.

Cross-linking time(hour)	Average fiber diameter $\pm$ SD (nm)
1	117 $\pm$ 12
3	122 $\pm$ 19
24	160 $\pm$ 23
Neat PVA	100 $\pm$ 17

Figure 4.3. represents the ATR FT-IR spectrum of neat PVA fibers and 1, 3, 24 hours cross linked PVA electrospun nanofibers. Neat PVA fibers clearly shows the presence of hydroxyl groups on the polymer chain as it shows characteristic vibrational bands at  $3350\text{ cm}^{-1}$ . After 1, 3, and 24-hour cross linking, the intensity of hydroxyl group was decreased at  $3570\text{-}3050\text{ cm}^{-1}$  when compared with neat PVA fibers. It refers that the -OH group in PVA interact with the -CHO group in glutaraldehyde (GA). Besides, it can be seen that the intensity of hydroxyl groups between 1, 3, and 24 hours cross linked PVA nanofibers has no obvious difference. The absorbance in  $2741$ , and  $2873\text{ cm}^{-1}$  refers to the aldehyde groups, and the generation of acetal ring and ether linkage due to the interaction between the aldehyde groups and hydroxyl groups causes the increment on absorbance between  $985$  and  $1362\text{ cm}^{-1}$ . Table 4.1 shows the Characteristics of before and after cross linking of PVA electrospun nanofibers.

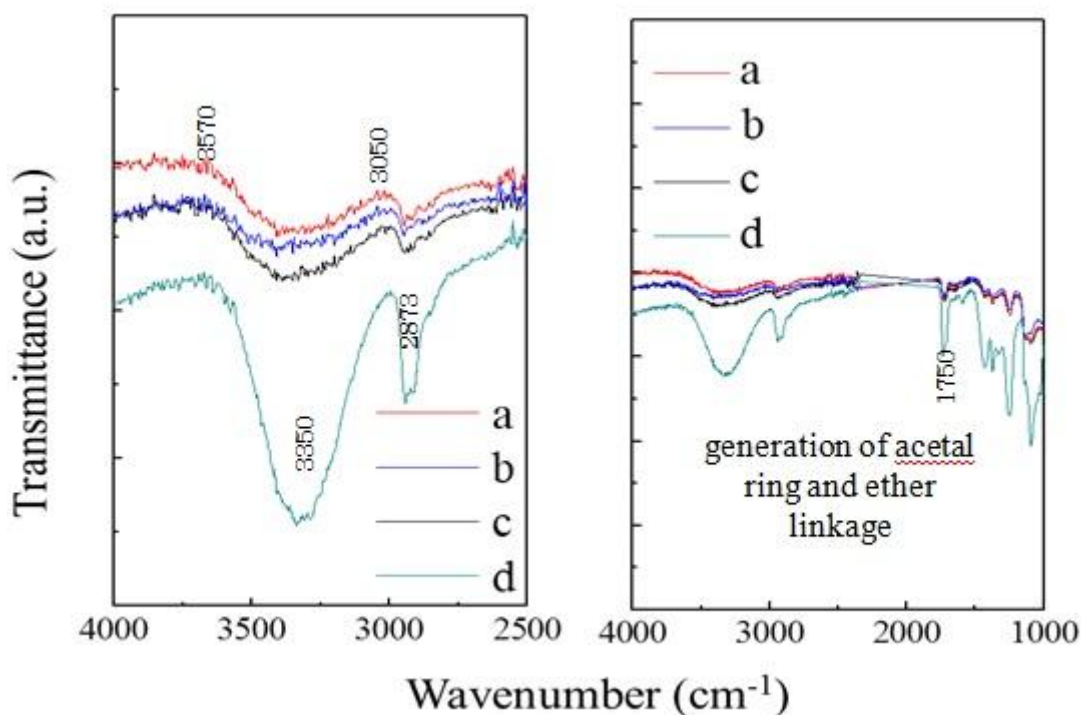


Figure 4.3. ATR FT-IR spectrum of PVA cross-linked nanofibers, a) 3 h, b) 24 h, c) 1 h, d) neat PVA nanofibers.

#### 4.2. PVA coating of pencil graphite electrode

By using conductive properties of graphite, we coated the surface of pencil electrode with PVA nanofibers by electrospinning process (Figure 4.4). 1, 2 and 5 min of PVA coating time was studied under the applied voltage of 28 kV, flow rate of 4 ml/h and 25 cm of tip to collector distance. SEM results of 8, 24 and 31  $\mu\text{m}$  fiber thickness after PVA fiber coating process of 1, 2, and 5 min respectively shows that there is no a linear correlation between the fiber thickness versus coating time (Figure 4.5). When the thickness of PVA nanofibers increased, it results a decrease in the fiber deposition amount and graphite conductivity due to the non-conductive nature of the PVA.



Figure 4.4. Photographic image of a) bare pencil graphite electrode, b) PVA coated pencil graphite electrode

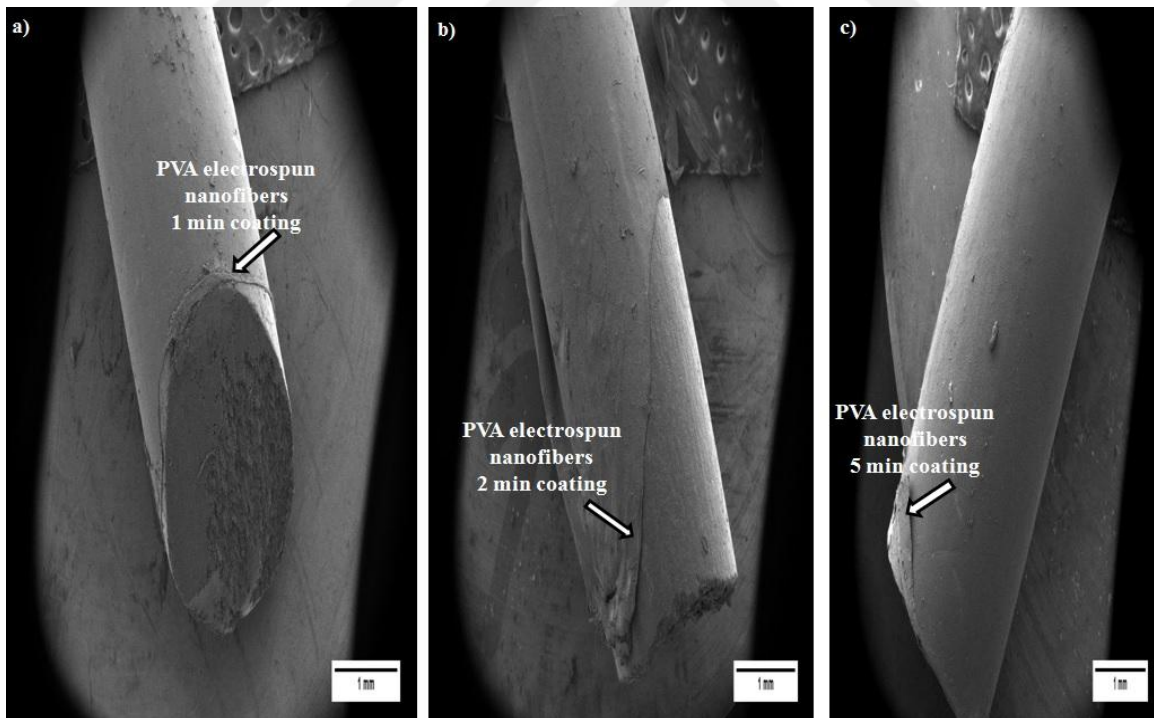


Figure 4.5. SEM micrograph of 1 min (a), 2 min (b) and 5min (c) coating of pencil graphite electrode

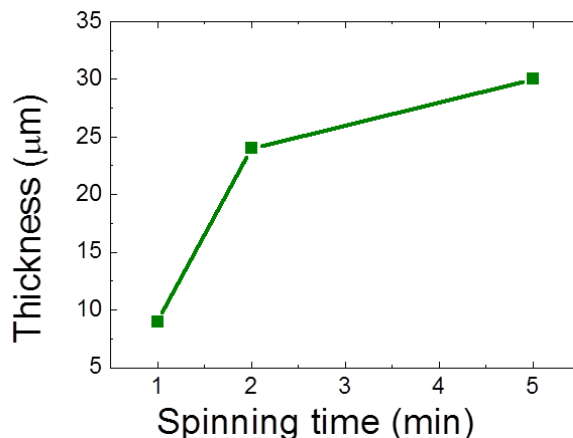
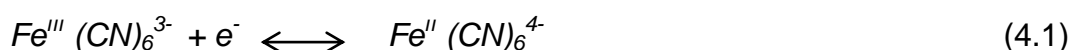


Figure 4.6. Correlation between PVA spinning time and fiber coating thickness on the surface of electrode.

### 4.3. Electrochemical Characterization

For evaluating the electro activity of the functionalized electrodes based on the fiber thickness and the PVA coating uniformity, cyclic voltammetry (CV) method was applied. CV method was carried out by investigating the electrodes in a solution of 50 mM  $\text{Fe}(\text{CN})_6^{3-/4-}$  containing 1 mM potassium chloride at a scan rate of 100 mV/s and between -100 mV and 650 mV scanning potentials. Figure 4.6 shows the cyclic voltammograms of PVA electrospun nanofiber coated pencil graphite electrode and bare pencil graphite electrode. Thinking the electrode reaction of ferricyanide is decreased to ferrocyanide (Eq.4.2), the peak current, which is expressed as  $I_p$  is controlled by the equation named Randle-Sevcik. In the equation, the  $k = 2.72 \times 10^5$ ,  $n$  refers to the number of moles of transferred electrons,  $A$  refers to the area of the electrode in  $\text{cm}^2$ ,  $D$  refers to the diffusion coefficient in  $\text{cm}^2/\text{s}$ ,  $C^b$  refers to the concentration of solution in M and  $v$  refers to the scan rate of the potential (volts/s).



$$I_p = k n^{3/2} A D^{1/2} C^b v^{1/2} \quad (4.2)$$

A redox peak pairs at 77.3  $\mu\text{A}$  and -77.3  $\mu\text{A}$  current values was achieved for the bare pencil graphite electrode. The peak current was reduced to 0.35  $\mu\text{A}$  and -0.35  $\mu\text{A}$  after 1 min of PVA nanofiber coating while the value was reduced to 0.29



$\mu\text{A}$  and  $-0.29 \mu\text{A}$  after coating for 2 min and finally it was reduced to  $0.029 \mu\text{A}$  and  $-0.029 \mu\text{A}$  after 5 min of PVA nanofiber coating. Non-conductive nature of the PVA results an obstructed electron transfer, and consequently a decreased potential. The reason for the significant decrease in peak potential can be explained by the Randle-Sevcik equation (4.2). Transferred number of moles of electrons ( $n$ ) is one of the prominent parameter for the PVA modified species, And the other parameter is the area of the electrode surface ( $A$ ). The PVA nanofibers repress the effective electron transfer to the surface of pencil graphite electrode compared to bare graphite electrode. Consequently, results a significant decrease in peak potential.

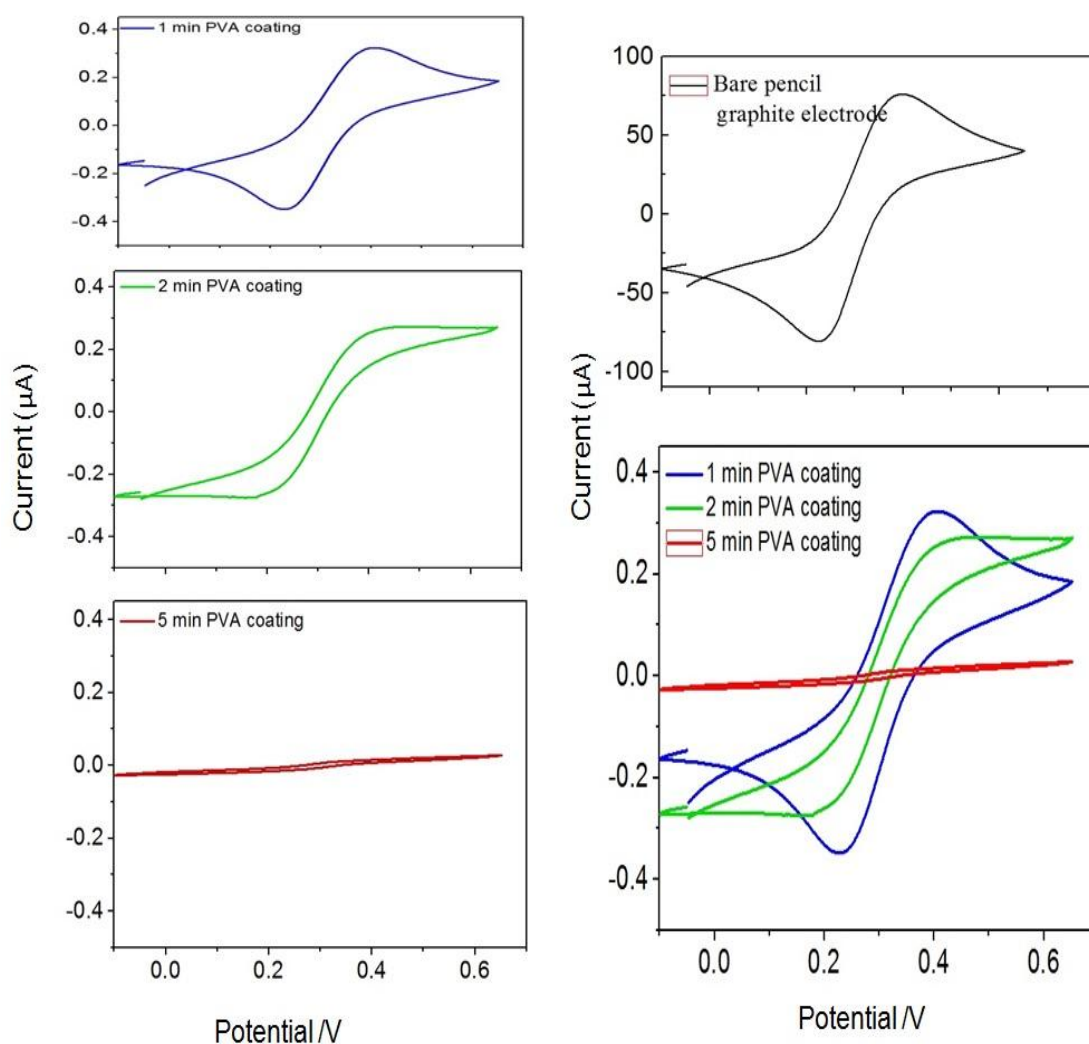


Figure 4.7. Cyclic voltammograms of PVA nanofiber coated pencil graphite electrode and bare pencil graphite electrode in  $50 \text{ mM Fe(CN)}_6^{3-/4-}$  in  $1 \text{ mM}$  potassium chloride.

The correlation between the fiber mat thickness on the surface of electrode, PVA spinning time, and peak current is achieved (Figure 4.7). For evaluating the interface characteristics of PVA nanofiber coated pencil graphite electrode, Electrochemical impedance Spectroscopy (EIS) experiments were carried out applying the AUTOLAB PGSTAT204 Compact and modular potentiostat/Galvanostat. The dielectric and insulating characteristics of the electrode system influences the electron transfer resistance value  $R_{ct}$  (semicircle diameter). The increase in  $R_{ct}$  which is caused by coating the surface of the electrode results an increase in resistance of electron transfer.

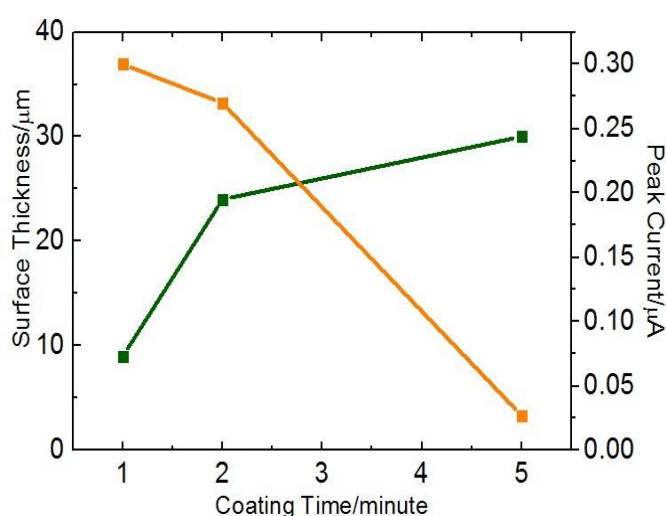


Figure 4.8. Correlation between the fiber mat thickness, coating time and peek current.

Figure 4.8 shows the Nuquist plots of the EIS of bare and PVA nanofiber coated pencil graphite electrode. On the graph in Figure 4.8,  $Z''$  refers to the real variable and  $Z'$  is the negative value of the imaginary variable of impedance. Figure 4.8 a) 1 min PVA nanofiber coated pencil graphite electrode shows enhanced semicircle diameter rather than bare pencil graphite electrode. It conforms the largest electron transfer resistance because of the insulating effect of PVA layer. Figure 4.8 b-c) 2 and 5 min PVA nanofiber coated pencil graphite electrode shows more increased electron transfer resistance and hereby an increase at  $R_{ct}$  value in the order of bare < 1 min < 2 min < 5 min.

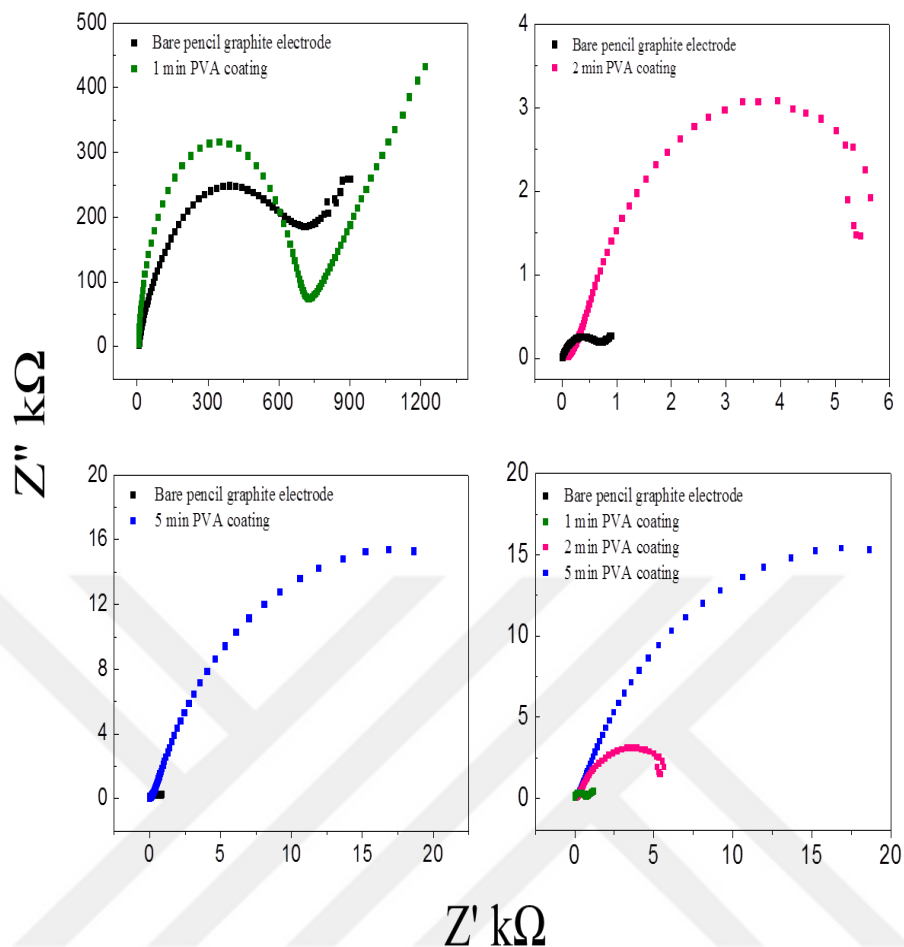


Figure 4.9. Electrochemical Impedance Spectra of PVA coated pencil graphite electrode and bare pencil graphite electrodes in 10 mM  $\text{Fe}(\text{CN})_6^{3-/4-}$  solution in 0.2 mM potassium chloride.

#### 4.4 Characterization of PVA/CNT composite nanofiber mats

Figure 4.9 shows the Cyclic voltammograms of uncovered pencil graphite electrode (PGE), PVA electrospun nanofiber coated pencil graphite electrode (PGE/PVA), MWCNT functionalized PVA nanofiber coated PGE (PGE/PVA-MWCNT), and interfacial cross-linked PVA functionalized with MWCNT coated pencil graphite electrode. Cyclic voltammetry (CV) measurements were carried out in 1 M  $\text{KNO}_3$  and 50 mM  $\text{K}_3[\text{Fe}(\text{CN})_6]$  at a scan rate of  $100 \text{ mVs}^{-1}$  for the redox couple reaction which is reversible at  $-0.1 \text{ V}$  to  $0.6 \text{ V}$  versus  $\text{Ag}/\text{AgCl}$ . The oxidation current response for PGE/PVA was observed as  $24 \mu\text{A}$  while the value

was enhanced to 49  $\mu\text{A}$  for PGE/PVA-MWCNT. Carbon nanotubes separated inside and outside surface of the electrospun nanofibers during the process of nanofiber fabrication. CNTs which were located inside surface of the electrospun nanofibers are insulated due to the non-conductive PVA layer. It indicates that 4 wt % total mass effect of applied MWCNT does not contribute to the nanofiber conductive characteristics, and besides, the electrospinning performance of PVA solution limited by the enhancing content of CNT. It is also observed that two times higher current response for the interfacial cross-linked PVA functionalized with MWCNT coated pencil graphite electrode was observed compared to PGE/PVA-MWCNT electrode.

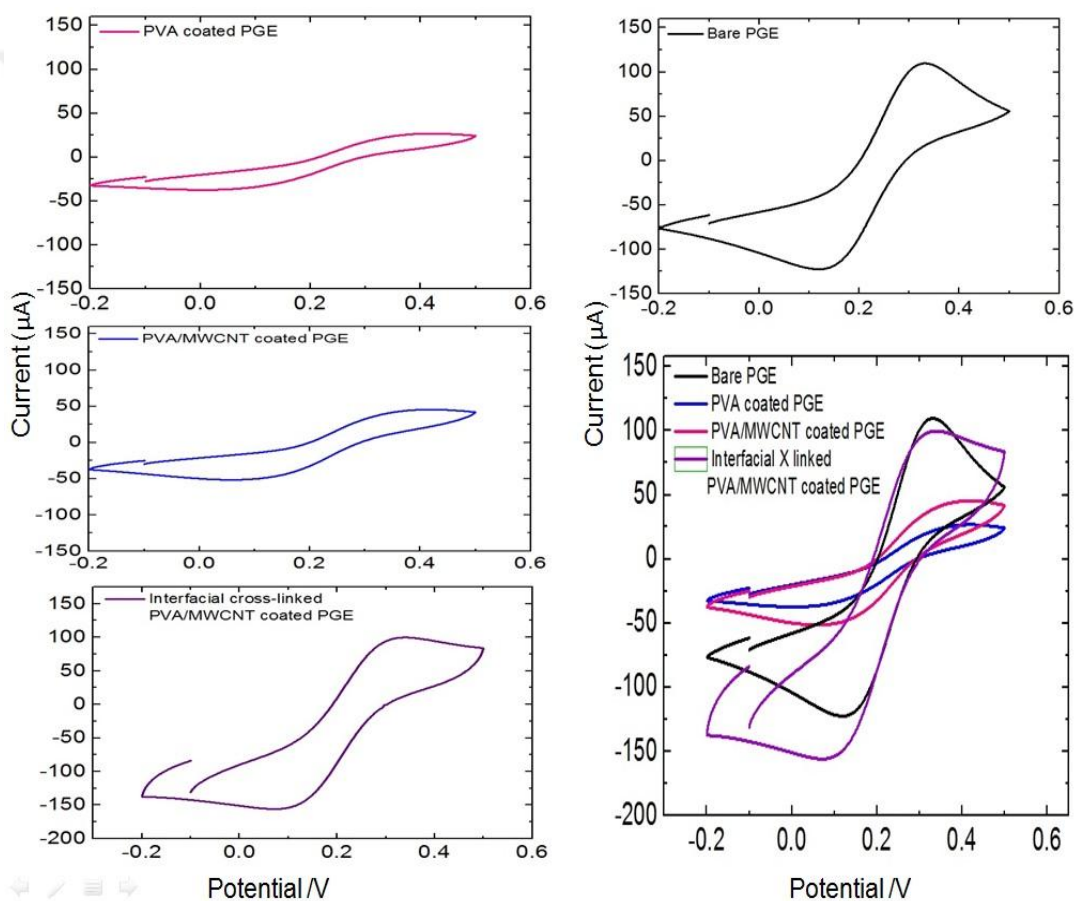


Figure 4.10. Cyclic voltammograms of bare PGE, PVA electrospun nanofiber coated PEG, PVA/MWCNT-PEG and interfacial cross-linked PVA/MWCNT-PEG.

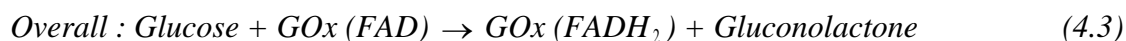
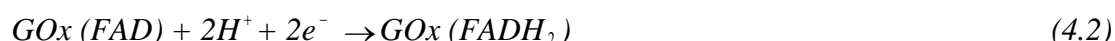
## 4.5. Enzyme Electrodes

### 4.5.1. Glucose sensing activities of the enzyme electrodes

PDDA functionalized MWCNT results an increased dispersion of modified CNTs in PVA matrix. As there is a positive charge on protonated nitrogen in the chains of PDDA that creates the electrostatic repulsive forces among the MWCNTs which was functionalized with PDDA, and at the same time prevents the aggregation of CNT. Consequently, GOx electrostatically links to the CNTs surface as GOx is negatively charged in pH 7.4.

Comparative glucose sensing activity of the electrodes were measured amperometrically with injection of glucose at an applied voltage at - 0.5 V. Six different electrodes was prepared for this study such as a) *uncovered pencil graphite electrode*, b) *GOx immobilization of PVA electrospun electrode*, c) *GOx immobilization of PVA electrospun electrode functionalized with MWCNT*, d) *GOx immobilization of PVA electrospun electrode functionalized with PDDA modified MWCNT*, e) *GOx immobilization of PVA electrospun electrode functionalized with PDDA modified SWCNT*, f) *GOx immobilized, Interfacially cross-linked PVA electrospun electrode functionalized with PDDA modified MWCNT*.

For controlling the physical constancy of three electrodes electrochemical cell system, the uncovered pencil graphite electrode (neither GOx nor AOx was immobilized on its surface) was applied as control electrode. Considering of the reaction between FADs and glucose (reaction 4.1-4.3), the successive injection of glucose results a decrease of FAD (reaction 4.2) and an increase on FADH<sub>2</sub> concentration and hereby oxidation of FADH<sub>2</sub> (reverse reaction of 4.2). Therefore, an in-situ injection of glucose, usually to the medium containing GOx, causes an increment on peak current, and this increment is directly proportional to the glucose concentration.



However, the current response was enhanced non-linearly, and the regression value of the linear function for uncovered pencil graphite electrode is observed as 0.0292 (Figure 4.10). It means that there is no agreement between current response versus concentration of glucose, and this random and non-linear dispersion of current response resulted from the nonexistence of GOx in the reaction medium, and the increment between -15  $\mu\text{A}$  and -21  $\mu\text{A}$  may cause from the physical imbalance of three electrodes electrochemical system.

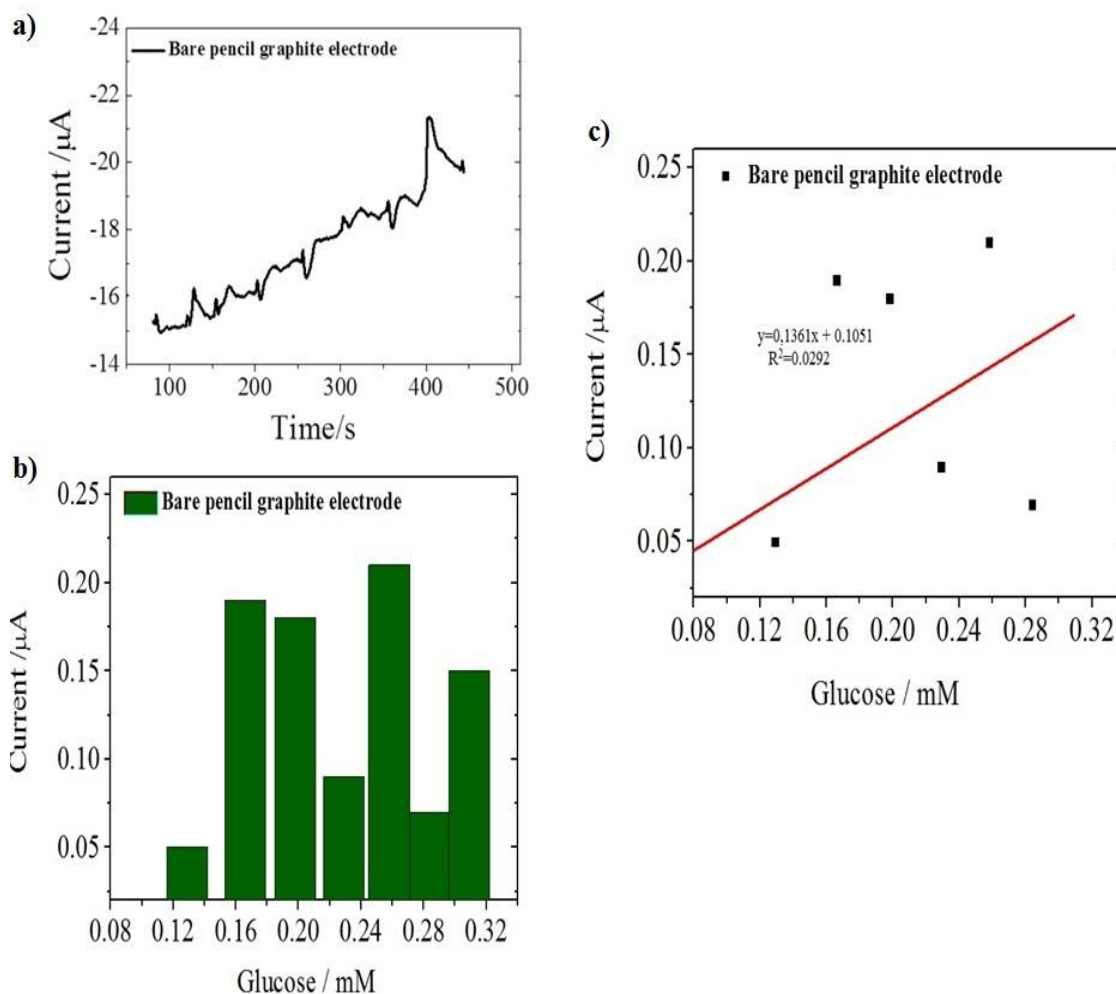


Figure 4.11. a) Chronoamperometric response of GOx bare pencil graphite electrode for the successive injection of 1mM glucose in a stirred 0.1 M PBS (pH 7.4) with -0.5 V Potential, b) correlation between glucose concentration and current response, c) Calibration curve

A smooth increase of approximately 1  $\mu\text{A}$  was achieved for the current response after injecting of each 1 mL of 1 mM glucose, and thereafter a reduction was observed with showing difference of 0.50  $\mu\text{A}$  for the current response (Figure 4.11). Detaching of GOx molecules from the surface of PVA electrospun nanofiber may occurred in the stirring aqueous medium, and consequently induces this decrease on current response. The other effects contributed to this reduction might arise from the non-conductive nature of PVA membrane that induces obstructed electron transfer between the electrode versus the enzyme. Linear function of the observed calibration curve does not exhibit correlative behaviour between current response versus concentration of glucose. The regression value of the linear function is observed as 0.6512, and the glucose sensing limitation of the electrode was achieved as 0.0476 mM.

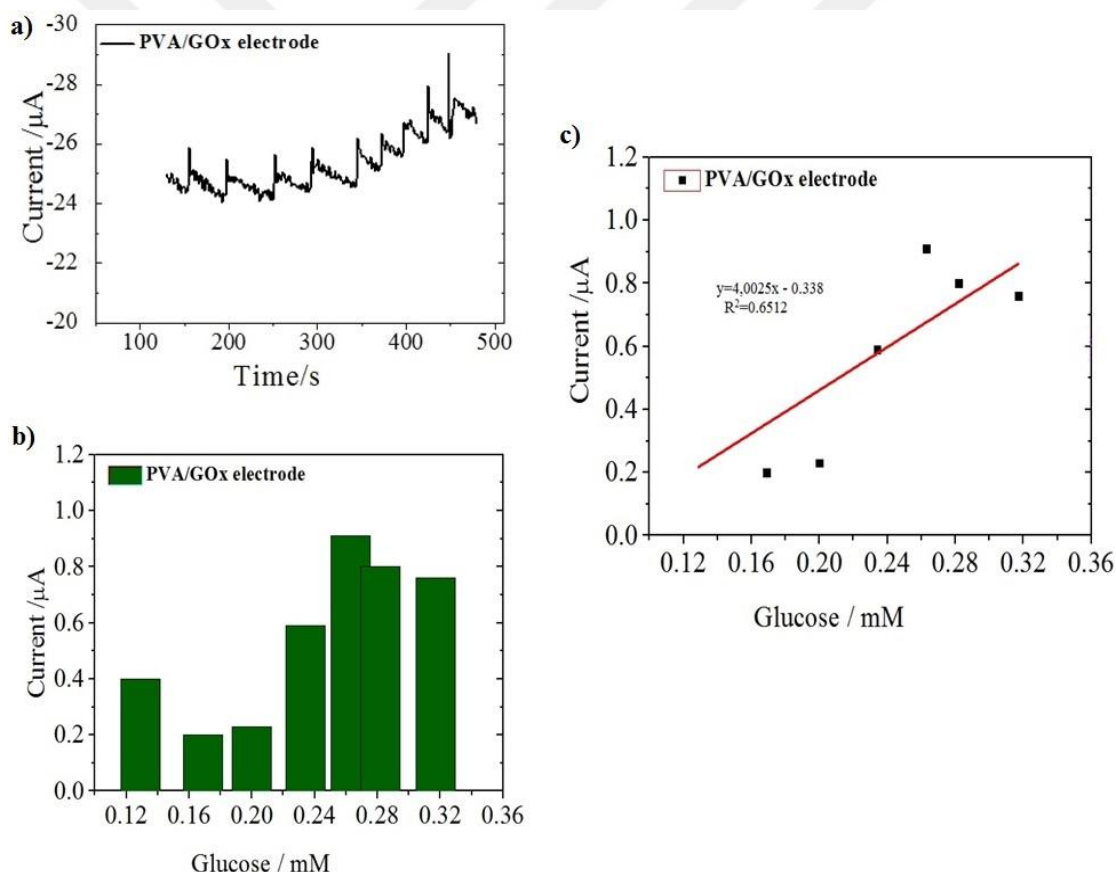


Figure 4.12. a) Chronoamperometric response of GOx immobilization of PVA electrospun electrode for the successive injection of 1mM glucose in a stirred 0.1 M PBS (pH 7.4) with -0.5 V Potential, b) correlation between glucose concentration and current response, c) Calibration curve.

For evaluating the effect of CNTs on GOx catalytic reactivity, amperometric measurements were carried out for the GOx immobilization of PVA electrospun electrode functionalized with MWCNT. Figure 4.12 a) shows the amperometric response of GOx immobilization of PVA electrospun electrode functionalized with MWCNT for the injection of 1 mM glucose in a stirred 0.1 M PBS (pH 7.4) with -0.5 V Potencial, b) correlation between glucose concentration and current response, c) Calibration curve.

An increment of nearly 2  $\mu\text{A}$  of current value was observed after the injection of each 1 mM and 1mL solution of glucose. The current response reached its steady state value with difference of approximately 1  $\mu\text{A}$ . It is observed from the data that modification with MWCNT does not effectively increase the enzyme electrode catalytic reactivity. It is achieved that the response time of the electrode was nearly 15 s and the sensing limitation of this electrode was achieved as 0.0476 mM, besides, it is observed that there was no correlation between current increment versus increasing concentration of glucose and the regression values of the linear function for the electrode is observed as 0.7461. Enzyme electrode prohibits an analogy with the previous GOx immobilization of PVA electrospun electrode even though the existence of MWCNT. This inefficiency might caused from the lower adsorption value of the GOx molecules onto the CNTs surface. And this weak adsorption value can arise from the negative charges on the CNTs carboxylated surface that cause a repulsive effect on GOx as it is negatively charged at pH 7.4, and hereby results a reduced adsorption value of GOx onto the surface of MWCNT.



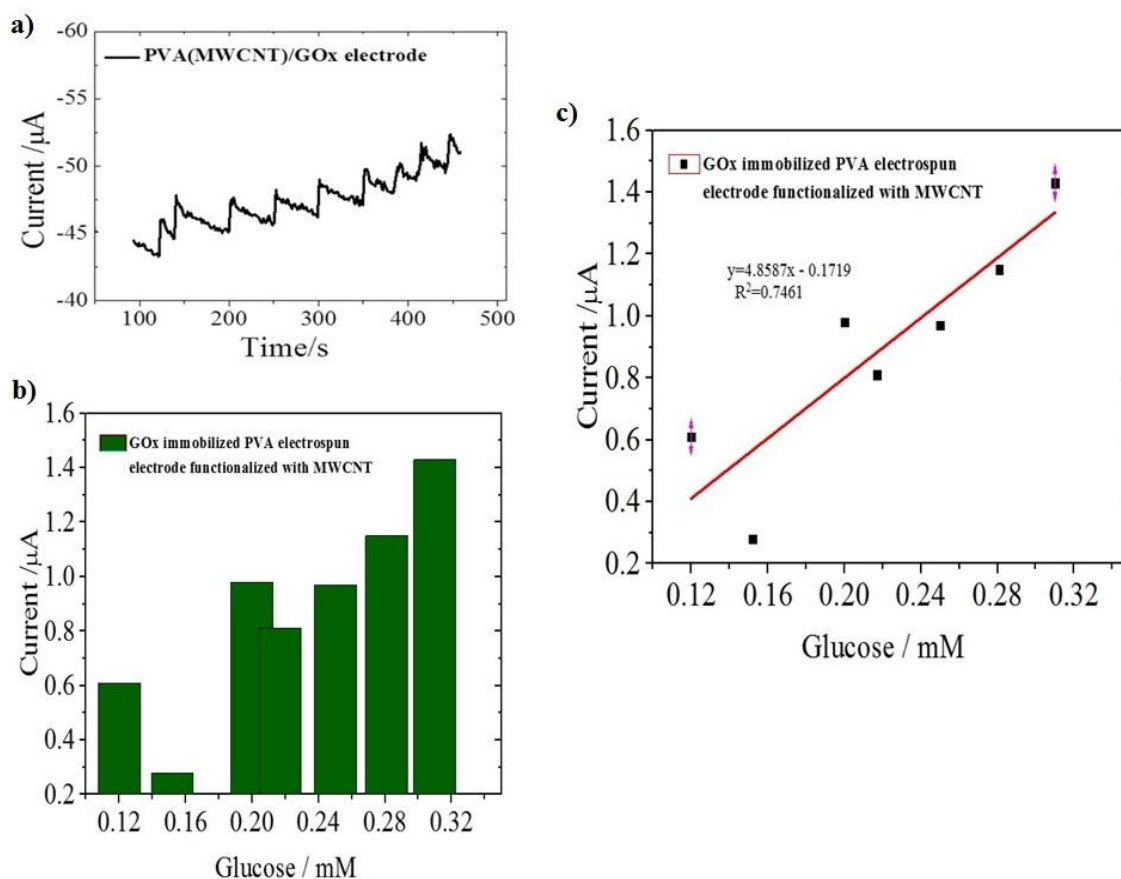


Figure 4.13. a) Chronoamperometric response of GOx immobilized PVA electrospun electrode modified with MWCNT for the successive injection of 1mM glucose in a stirred 0.1 M PBS (pH 7.4) with -0.5 V Potential, b) correlation between glucose concentration and current response, c) Calibration curve

For increasing the adsorbing efficiency of GOx onto the surface of CNT, functionalized CNTs modified with the Poly(diallyldimethylammonium) chloride (PDDA). Figure 4.13 shows the amperometric response of GOx immobilization of PVA electrospun electrode functionalized with PDDA modified MWCNT (a), and correlation between glucose concentration and current response (b), and resulting calibration curve (c). It is obvious from the data that the current response enhance nearly 1  $\mu\text{A}$  for the each injection of glucose in 1 mM and 500  $\mu\text{L}$  volume. And the time for reaching steady state value of current response is observed as 26s. Glucose sensing limit of this electrode is obtained as 0.0243 mM. The regression value of the linear function is observed as 0.8974. It means the greater correlation between glucose concentration and current response.

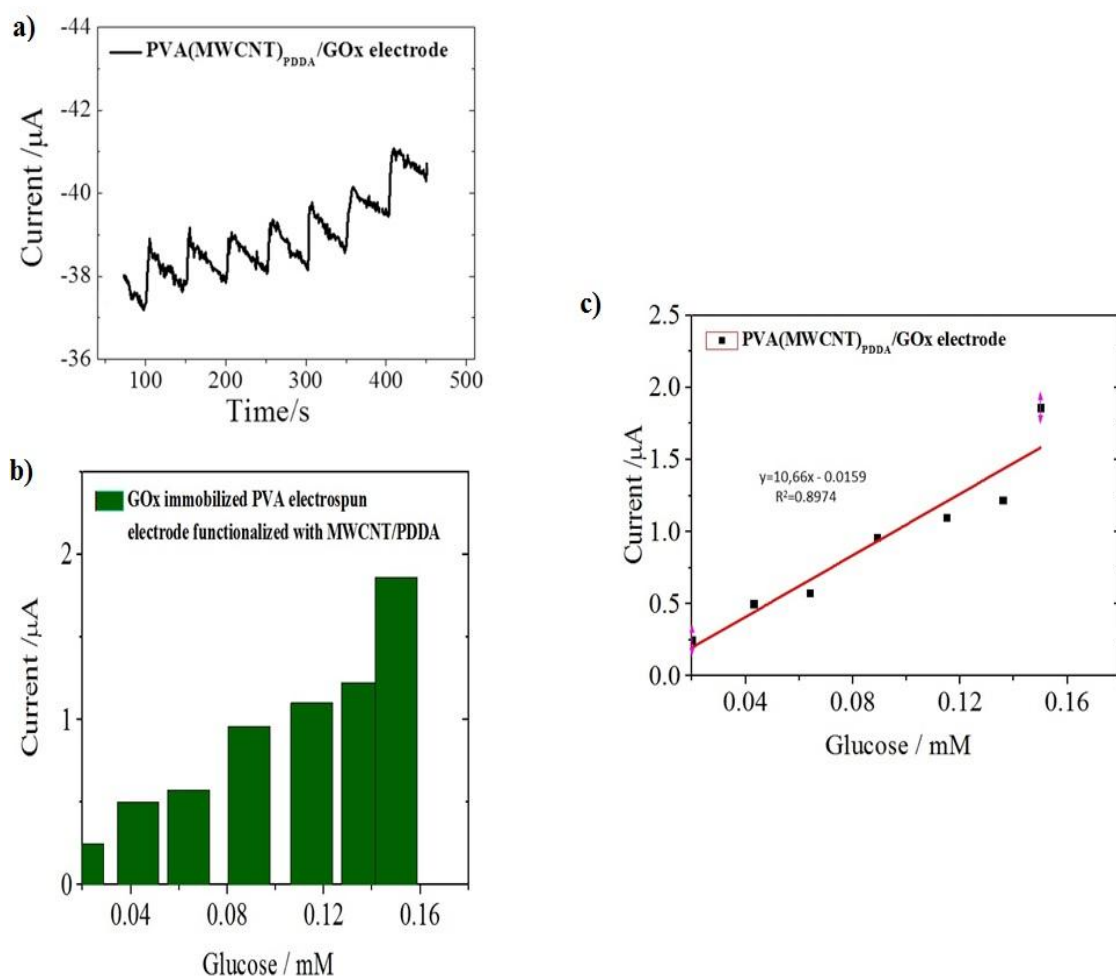


Figure 4.14. a) Chronoamperometric response of GOx immobilized PVA electrospun electrode functionalized with MWCNT/PDDA for the successive injection of 1mM glucose in a stirred 0.1 M PBS (pH 7.4) with -0.5 V Potential, b) correlation between glucose concentration and current response, c) Calibration curve.

For detecting the influence of CNT types on the catalytic reactivity of GOx, chronoamperometric response of GOx immobilization of PVA electrospun electrode functionalized with PDDA modified SWCNT for the glucose addition was achieved (Figure 4.14.a). The correlation between current response and glucose concentration is shown in (b), and resulting calibration curve is shown in (c). It is achieved from the data that the current response enhanced nearly 1  $\mu\text{A}$  for each injection of glucose in 1 mM and 500  $\mu\text{L}$  volume. And the time for reaching steady

state value of current response is observed as 19 s. Glucose sensing limit of this electrode is obtained as 0.0243 mM. The regression value of the linear function is observed as 0.9102. It means the greater correlation between glucose concentration and current response. The current response does not show a reduction compared with the previously analyzed four electrodes.

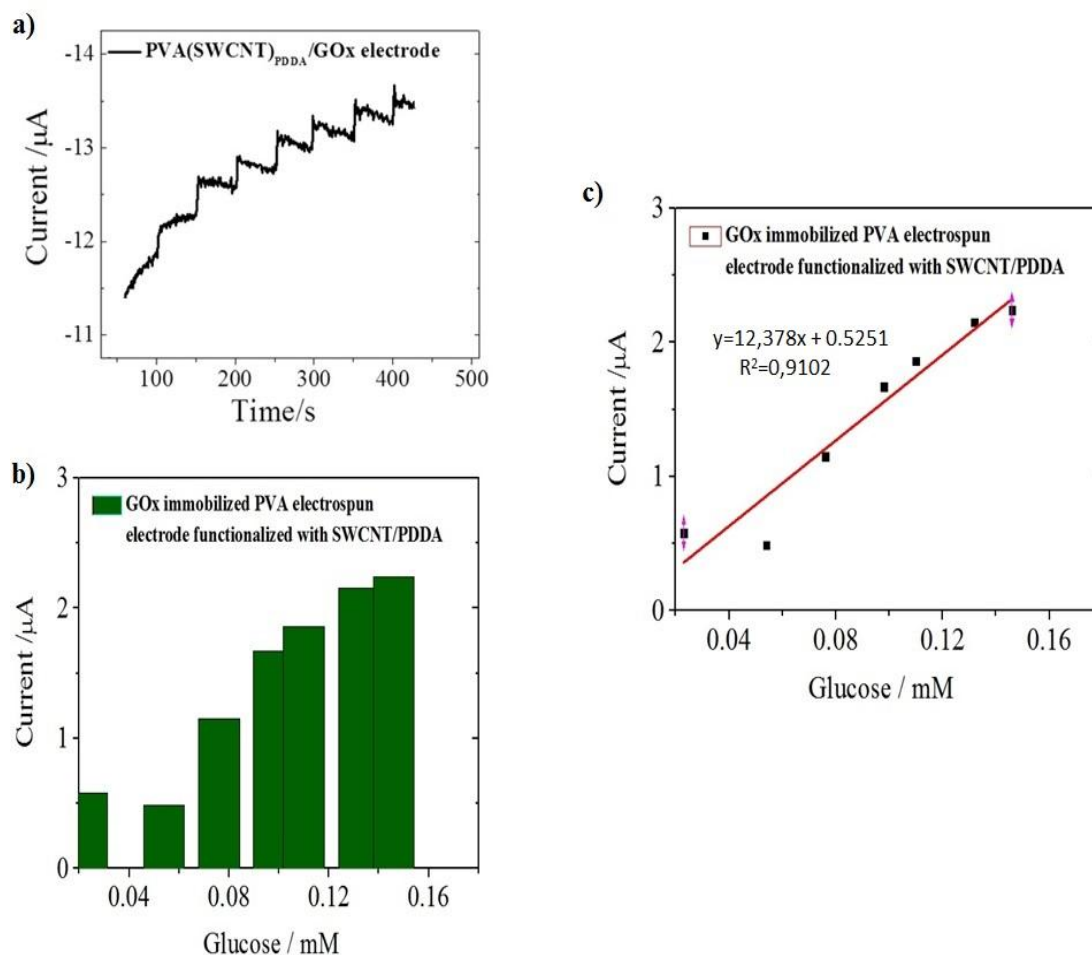


Figure 4.15. a) Chronoamperometric response of GOx immobilized PVA electrospun electrode functionalized with SWCNT/PDDA for the successive injection of 1mM glucose in a stirred 0.1 M PBS (pH 7.4) with -0.5 V Potencial, b) correlation between glucose concentration and current response, c) Calibration curve

Finally, for detecting the influence of CNT modification to the surface of PVA fibers, amperometric response of GOx immobilized and interfacially cross-linked PVA electrospun electrode functionalized with PDDA modified MWCNT for the glucose

injection was studied (Figure 4.15.a). The correlation between current increment and glucose concentration is shown in (b), and resulting calibration curve is shown in (c). It is achieved from the data that the current response shows a sharp enhancement for the addition of 1 mM glucose. And the time for reaching steady state value of current response is observed as 12 s. Glucose sensing limit of this electrode is obtained as 0.1 mM. The regression value of the resulted linear function is observed as 0.958. It means much greater correlation between the concentration of glucose and current response. With the increase of glucose concentration, the current response shows a gradual increase.

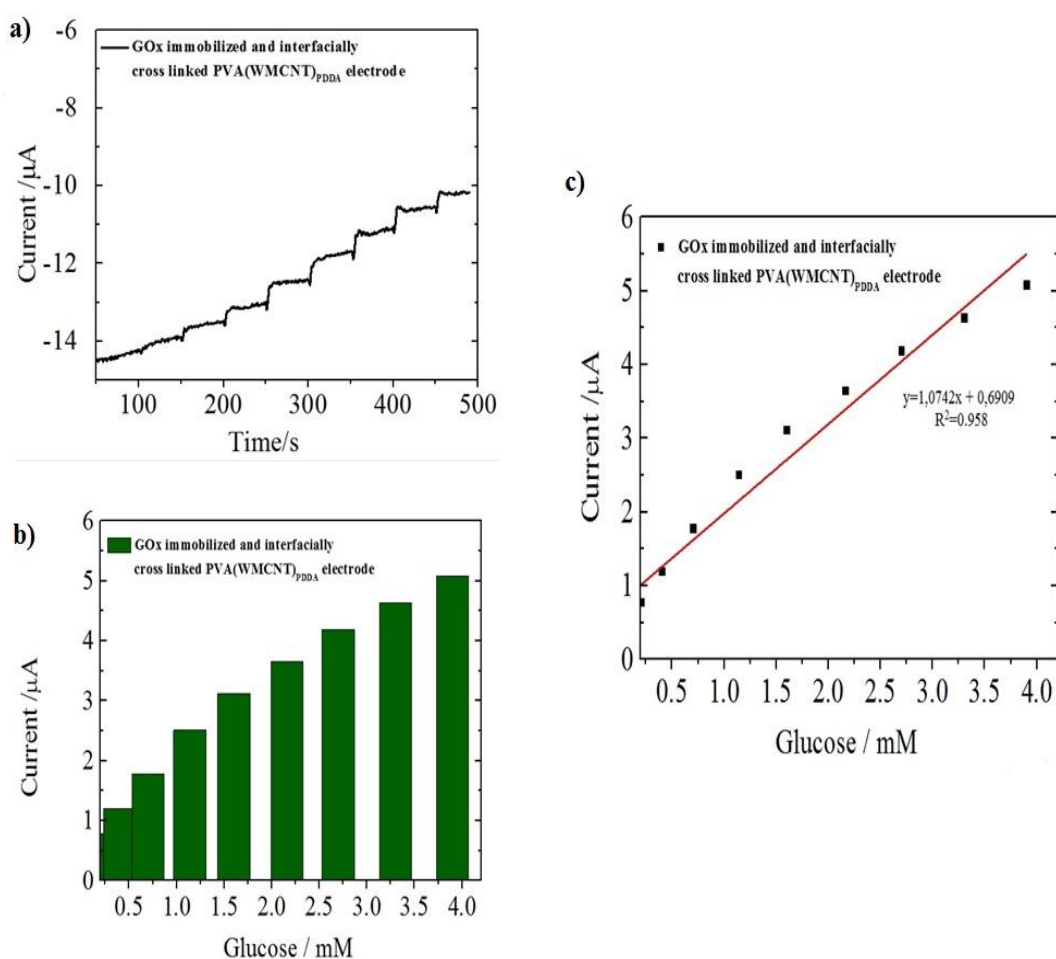


Figure 4.16. a) Chronoamperometric response of Interfacially cross-linked PVA electrospun electrode containing PDDA functionalized MWCNT at an applied Potential of -0.5 V to successive addition of 1mM glucose in a stirred 0.1 M, pH 7.4 PBS, b) Relationship between curve

Calculations about the electrode surface area which was exposed to the catalytic reaction was carried out based upon the cylinder dimensions with 0.9 mm in diameter and 10 mm in height. Table 4.2 shows the sensitivities of five different electrodes after calculation.

Table 4. 2 Calculated sensitivities of five different enzyme electrodes.

Type of Enzyme Electrodes	Sensitivity ( $\mu\text{A mM}^{-1}\text{cm}^{-2}$ )
GOx immobilized PVA electrospun electrode	19.4
GOx immobilized PVA electrospun electrode functionalized with MWCNT	25.9
GOx immobilized PVA electrospun electrode functionalized with PDDA modified MWCNT	65.8
GOx immobilized PVA electrospun electrode functionalized with PDDA modified SWCNT	42.7
GOx immobilized and interfacially cross-linked PVA electrospun electrode functionalized with PDDA modified MWCNT	4.01

Detectivity of GOx immobilization of PVA electrospun electrode was calculated as  $19.4 \mu\text{A mM}^{-1}\text{cm}$ , and after functionalization with MWCNT, sensitivity of the enzyme electrode is reached to  $25.9 \mu\text{A mM}^{-1}\text{cm}$ . GOx binding efficiency onto the surface of PVA electrospun membrane may be restricted because of the unmodified behavior of pristine PVA fiber surface. The electron transfer efficiency was resisted because of the non-conductive nature of the PVA fiber membrane. Functionalized MWCNT surface shows a negatively charged layer which resists the linking efficiency of GOx. Consequently, the enhancement on enzyme binding efficiency may not be caused by the addition of MWCNT. However, in consideration of the immobilized GOx molecules, CNT may attribute to the electron transfer efficiency of the electrode. Accordingly, the glucose sensitivity of the GOx immobilization of PVA electrospun electrode functionalized with PDDA modified MWCNT was observed as  $65.8 \mu\text{A mM}^{-1}\text{cm}$  that shows much higher sensitivity compared to the GOx immobilization of PVA electrospun electrode functionalized with PDDA modified SWCNT ( $42.7 \mu\text{A mM}^{-1}\text{cm}$ ). This much higher sensitivity of this enzyme

electrode can be explained with the electrostatic interactions among PDDA versus negatively charged GOx. Glucose sensing efficiency of GOx immobilized and interfacial cross-linked PVA electrospun electrode functionalized with PDDA modified MWCNT was observed as  $4.01 \mu\text{A mM}^{-1}\text{cm}$  which shows the lowest value compared with other enzyme electrodes. This decrease can be explained by the increased fiber diameter of interfacially cross-linked PVA electrospun nanofibers rather than pristine PVA electrospun nanofiber (312 and 100 nm) that may result a reduced surface area arised from the enhanced fiber diameter for GOx for binding to the electrode surface, and hereby results an inefficient sensing efficiency for the sensor electrode which was interfacially cross-linked. Considering of the electrical characteristics of CNTs, all the results obtained are consistent with the literatures.

It is reported that the electron transfer activity of the graphite-like materials occurs at surface defect regions, and constitutively occurs at edge-plan-like sites [67]. It has been studied from the researches that the pyrolytic graphite surface defects demonstrate higher electron transfer efficiency constant (k) rather than its basal plane, furthermore the electron transfer rate constant of defect free regions of pyrolytic graphite surface which is in forms of exposed edge plane nanobands is nearly zero [68]. Besides, it is reported from the studies that the enhanced defect ratio refers to the open end surface of carbon nanotube, which had an increased charge transfer rate, consequently has an enhanced electrocatalytic activity [69]. The greater glucose sensing efficiency of GOx immobilized PVA electrospun electrode functionalized with PDDA modified MWCNT might be arise from the higher charge transfer rate of functionalized MWCNT. Researchers have been immobilized enzymes onto the surface of Au electrode for fabricating amperometric glucose sensing biosensors. These studies reported that the glucose sensing electrodes demonstrate a rapid response and higher current response for the successive addition of glucose [70].

## 5. CONCLUSIONS

In our study, we have fabricated a glucose biosensor by applying electrospinning technique, and PVA was used during the procedure of electrospun nanofibers fabrication.

Detecting efficiency of the sensor electrodes was controlled by using the effective parameters like PDDA, different types of CNT and functionalized CNTs. Different types of carbon nanotubes were purified and oxidized with acid treatment. Developed PVA nanofiber membranes was modified with acid treated different types of CNTs and interfacial cross-linking. 1,3 and 24 h cross-linking results were evaluated by Scanning Electron Microscope (SEM) and ATR FT-IR measurements were carried out before and after cross-linking of electrospun nanofibers. Average fiber diameter for neat PVA nanofibers is observed as 100 nm, and this value is increased to 117 nm for 1 h, 122 nm for 3 h, and 160 nm for 24 h of cross-linking. GOx was physically linked onto the surface of CNTs by using cationic polymer PDDA. GOx immobilized PVA sensor electrode shows 0.048 mM of glucose detection limit and  $19.4 \mu\text{A mM}^{-1}\text{cm}^{-2}$  of sensitivity. After modifying with MWCNT, a relatively higher sensitivity of  $25.9 \mu\text{A mM}^{-1}\text{cm}^{-2}$ , and the detection limit of 0.048 mM is observed for GOx immobilized PVA electrospun electrode functionalized with MWCNT. The highest sensitivity of  $65.8 \mu\text{A mM}^{-1}\text{cm}^{-2}$  is observed after modifying the surface of CNTs with cationic polymer PDDA for GOx immobilized PVA electrospun electrode Functionalized with PDDA modified MWCNT. Glucose detection limit for this sensor electrode is observed as 0.02 mM. This increment caused from the electrostatic interactions between the positively charged PDDA versus negatively charged GOx, and hereby results an increased GOx adsorption value, consequently higher glucose sensing activity. After applying SWCNT, the glucose sensitivity is decreased to  $42.7 \mu\text{A mM}^{-1}\text{cm}^{-2}$ , and the glucose detection limit is observed as 0.02 mM. However, the sensing efficiency of the sensor electrode which was interfacially cross-linked is observed as  $4.01 \mu\text{A mM}^{-1}\text{cm}^{-2}$  in spite of the greater surface conductivity rather than other sensor electrodes. Higher regression value of 0.958 and lower current response time of 12 s is observed for this sensor electrode. It means the greater correlation between glucose concentration and current response.

The glucose detection limit for this sensor electrode is observed as 0.1 mM. Considering the glucose concentration in the blood sample of diabetes patients, which is ranging from 2-30 mM, for our sensor electrodes containing PDDA functionalized SWCNT and MWCNT, the glucose detection limit is achieved as 0.02 mM. It means that our glucose sensing electrode shows suitable characteristics for detecting the glucose level in the blood sample of diabetes patients, and at the same time, it can be applied for increasing the glucose detecting efficiency of new developing systems.





## REFERENCES

- [1] N. Tolochko, "History Of Nanotechnology," *NANOSCIENCE AND NANOTECHNOLOGIES, Belarus*, **2009**.
- [2] H. Li, L. Songqing, Z. Dai, B. Jianchun and Y. Xiaodi, "Application of Nanomaterials in Electrochemical Enzyme Biosensors," *Sensors*, **2009**.
- [3] T. Bo, L. Cao and K. Xu, "A New Nanobiosensor for Glucose with High Sensitivity and Selectivity in Serum Based on Fluorescence Resonance Energy Transfer (FRET) between CdTe Quantum Dots and Au Nanoparticles," *Chemistry*, vol. 14, no. 12, pp. 1-8, **2007**.
- [4] X. Zhang, Q. Guo and D. Cui, "Nanoscience, nanotechnology and spectrometry", *Sensors*, Shanghai Jiao Tong University, 17 February 2009. Available: <https://doi.org/10.3390/s90201033>. **2014**.
- [5] S. Wild, G. Roglic, A. Green, R. Sicree and H. King, "Global Prevalence of Diabetes-Estimates for the year 2000 and projections for 2030," *Diabetes Care*, **2004**.
- [6] S. Pandit, D. Dasgupta, N. Dewan and P. Ahmed, "Nanotechnology based biosensors and its application," *The Pharma Innovation Journal*, vol. 5, no. 6, pp. 18-25, **2016**.
- [7] B. Kuswandi, "A Simple Visual Ethanol Biosensor Based on Alcohol Oxidase Immobilized onto Polyaniline Film for Halal Verification of Fermented Beverage Samples," *Sensors*, vol. 14, no. 24, pp. 1-15, **2014**.
- [8] C.-H. Lin, G.-B. Lee, Y.-H. Lin and G.-L. Chang, "A fast prototyping process for fabrication," *Journal of Micromechanics and Microengineering*, vol. 11, no. 726, p. 726–732, **2001**.
- [9] O. Parlak, A. Tiwari, A. P. Turner and A. Tiwari, "Template-directed hierarchical self-assembly of graphene based hybrid structure for electrochemical biosensing," *Biosensors and Bioelectronics*, vol. 49, pp. 53-62, **2013**.
- [10] N. Laurent, R. Haddoub and S. L. Flitsch, "Enzyme catalysis on solid surfaces," *Trends in Biotechnology*, vol. 26, no. 6, pp. 328-337, **2008**.
- [11] M. F. H. Jr, "There's plenty of room at the bottom: nanoscience in geochemistry," *ELSEVIER*, vol. 66, no. 5, pp. 735-743, **2002**.
- [12] N. Bhardwaj and S. C. Kundu, "Electrospinning: A fascinating fiber fabrication technique," *Biotechnology Advances*, vol. 28, no. 3, pp. 325-347, **2010**.

- [13] M. Bognitzki, W. Czad, T. Frese and A. Schaper, "*Nanostructured Fibers via Electrospinning*," *Advanced Materials*, vol. 13, no. 1, pp. 1-3, **2001**.
- [14] Q. Hou, D. W. Grijpma and J. Feijen, "*Preparation of Interconnected Highly Porous Polymeric Structures by a Replication and Freeze-Drying Process*," *Journal of Biomedical materials research*, vol. 106, no. 4, p. 732–740, **2003**.
- [15] Y. Shin, M. Hohman, M. Brenner and G. Rutledge, "*Experimental characterization of electrospinning: the electrically forced jet and instabilities*," *Polymer*, vol. 42, no. 25, pp. 09955-09967, **2001**.
- [16] Z.-M. Huang and Y.-Z. Zhang, "*A review on polymer nanofibers by electrospinning and their applications in nanocomposites*," *Composites Science and Technology*, vol. 63, no. 15, pp. 2223-2253, **2003**.
- [17] W. E. Teo, M. Kotaki, X. M. Mo and S. Ramakrishna, "*Porous tubular structures with controlled fibre orientation using a modified electrospinning method*," *Nanotechnology*, vol. 16, no. 918, p. 918–924, **2005**.
- [18] C.-F. Huang and F.-C. Chang, "*Comparison of hydrogen bonding interaction between PMMA/PMAA blends and PMMA-co-PMAA copolymers*," *Polymer*, vol. 44, no. 10, pp. 2965-2974, **2003**.
- [19] N. Bhardwaj and S. C. Kundu, "*Electrospinning: A fascinating fiber fabrication technique*," *Biotechnology Advances*, vol. 28, no. 3, pp. 325-347, **2010**.
- [20] V. Li, A. Ogawa, T. Horikoshi and T. Saito, "*Micromechanics-based Durability Study of Polyvinyl Alcohol-Engineered Cementitious Composite (PVA-ECC)*," *Aci Materials Journal*, vol. 101, no. 3, pp. 242-248, **2004**.
- [21] M.-S. Khil, D.-I. Cha, H.-Y. Kim and I.-S. Kim, "*Electrospun Nanofibrous Polyurethane Membranes as Wound Dressing*," *Journal of Biomedical Materials Research Part B*, vol. 67, no. 49, p. 675– 679, **2003**.
- [22] B. Kim, H. Park, S.-H. Lee and W. M., "*Poly(acrylic acid) nanofibers by electrospinning*," *Materials Letters*, vol. 59, no. 7, pp. 829-832, **2005**.
- [23] D. H. Reneker and A. L. Yarin, "*Electrospinning jets and polymer nanofibers*," *Polymer*, vol. 49, no. 10, pp. 2387-2425, **2008**.
- [24] Dehai Liang, B. S. Hsiao and Benjamin Chu, "*Functional electrospun nanofibrous scaffolds for biomedical applications*," *Advanced Drug Delivery Reviews*, vol. 59, no. 14, pp. 1392-1412, **2007**.
- [25] T. Subbiah, G. S. Bhat, R. W. Tock and S. Parameswaran, "*Electrospinning of nanofibers*," *Journal of Applied Polymer Science*,

vol. 96, no. 2, pp. 557-569, **2005**.

- [26] S. Liao, B. Li, Z. Ma and H. Wei, "*Biomimetic electrospun nanofibers for tissue*," *Biomedical Materials*, vol. 1, no. 3, pp. 45-53, **2006**.
- [27] W. Feng and P. Ji, "*Enzymes immobilized on carbon nanotubes*," *Biotechnology Advances*, vol. 29, no. 13, p. 889–895, **2011**.
- [28] M. Misson, H. Zhang and B. Jin, "*Nanobiocatalyst advancements and bioprocessing applications*," *JOURNAL OF THE ROYAL SOCIETY INTERFACE*, vol. 12, no. 20, pp. 1-20, **2014**.
- [29] W.-E. Teo, R. Ina and S. Ramakrishna, "*Technological advances in electrospinning of nanofibers*," *SCIENCE AND TECHNOLOGY OF ADVANCED MATERIALS*, vol. 12, no. 16, pp. 1-20, **2011**.
- [30] S. M. Jafari, *Nanoencapsulation Technologies for the Food and Nutraceutical*, Elsevier Inc., **2017**.
- [31] A. K. S, P. Sanpui and K. Chatterjee, "*Fabrication of Poly(Caprolactone) Nanofibers by Electrospinning*," *Science and Education*, vol. 2, no. 4, pp. 62-66, **2014**.
- [32] J.MDeitzel, J.Kleinmeyer, DHarris and N. Tan, "*The effect of processing variables on the morphology of electrospun nanofibers and textiles*," *Polymer*, vol. 42, no. 1, pp. 261-272, **2001**.
- [33] TamerUyar and FlemmingBesenbacher, "*Electrospinning of uniform polystyrene fibers: The effect of solvent conductivity*," *Polymer*, vol. 49, no. 24, pp. 5336-5343, **2008**.
- [34] D. Tasis, N. Tagmatarchis, A. Bianco and M. Prato, "*Chemistry of Carbon Nanotubes*," *CHEMICAL REVIEWS*, vol. 106, no. 3, p. 1105–1136, **2006**.
- [35] T. M. Swage, B. Esser and J. M. Schnorr, "*Selective Detection of Ethylene Gas Using Carbon Nanotube-based Devices: Utility in Determination of Fruit Ripeness*," *Journal of Angewandte Chemie*, vol. 51, no. 23, pp. 5752-5756, **2012**.
- [36] V. N.Popov, "*Carbon nanotubes: properties and application*," *Material Science and Engineering*, **2003**.
- [37] J. Wang, "*Carbon-Nanotube Based Electrochemical Biosensors*," *Electroanalysis*, vol. 17, no. 1, pp. 1-14, **2005**.
- [38] K. BShelimov, R. OEsenaliev and A. GRinzler, "*Purification of single-wall carbon nanotubes by ultrasonically assisted filtration*," *Chemical Physics Letters*, vol. 282, no. 5-6, pp. 429-434, **1998**.

- [39] Y.-O. Im, S.-H. Lee and T. Kim, "*Utilization of carboxylic functional groups generated during purification of carbon nanotube fiber for its strength improvement*," Applied Surface Science, vol. 392, no. 13, pp. 342-349, **2017**.
- [40] L. Luca, A. Donato, S. Santangelo and G. Faggio, "*Hydrogen sensing characteristics of Pt/TiO<sub>2</sub>/MWCNTs composites*," International Journal of Hydrogen Energy, vol. 37, no. 2, pp. 1842-1851, **2012**.
- [41] T. Filleter and H. D. Espinosa, "*Multi-scale mechanical improvement produced in carbon nanotube fibers by irradiation cross-linking*," Carbon, vol. 56, no. 16, pp. 1-11, **2013**.
- [42] S. Ahmed Ansari and Qayyum Husain, "*Potential applications of enzymes immobilized on/in nano materials: A review*," Biotechnology Advances, vol. 30, no. 3, pp. 512-523, **2012**.
- [43] Long Zhao, Qingjie Liu, Shili Yan and Zhoujiang Chen, "*Multimeric immobilization of alcohol oxidase on electrospun fibers for valid tests of alcoholic saliva*," Journal of Biotechnology, vol. 168, no. 1, pp. 46-54, **2013**.
- [44] J. T. Cang-Rong and G. Pastorin, "*The influence of carbon nanotubes on enzyme activity and structure: investigation of different immobilization procedures through enzyme kinetics and circular dichroism studies*," Nanotechnology, vol. 20, no. 15, pp. 1-21, **2009**.
- [45] Chen-An Lee and Yu-Chen Tsai, "*Preparation of multiwalled carbon nanotube-chitosan-alcohol dehydrogenase nanobiocomposite for amperometric detection of ethanol*," Sensors and Actuators B: Chemical, vol. 138, no. 2, pp. 518-523, **2009**.
- [46] A. J. S. Ahammad, J.-J. Lee and A. Rahman, "*Electrochemical Sensors Based on Carbon Nanotubes*," Sensors, vol. 9, no. 2, pp. 2289-2319, **2009**.
- [47] T. J. McDonald, D. Svedruzic, Y.-H. Kim, J. L and Blackburn, "*Wiring-Up Hydrogenase with Single-Walled Carbon Nanotubes*," NANO LETTERS, vol. 7, no. 11, pp. 3528-3534, **2007**.
- [48] W. Feng and P. Ji, "*Enzymes immobilized on carbon nanotubes*," Biotechnology Advances, vol. 29, no. 3, p. 889–895, **2011**.
- [49] Q. Zhang, S. Wu and L. Zhang, "*Fabrication of polymeric ionic liquid/graphene nanocomposite for glucose oxidase immobilization and direct electrochemistry*," Biosensors and Bioelectronics, vol. 26, no. 15, p. 2632–2637, **2011**.
- [50] G. Ren, X. Xu and Q. Liu, "*Electrospun poly(vinyl alcohol)/glucose oxidase biocomposite membranes for biosensor application*," Reactive

- & Functional Polymers, vol. 66, no. 43, p. 1559–1564, **2006**.
- [51] B. E. P. SWOBODA V. MASSEY, "*Purification and Properties of the Glucose Oxidase*," THE JOURNAL OF BIOLOGICAL CHEMISTRY, vol. 240, no. 5, pp. 2209-2215, **1965**.
- [52] Cash, Kevin J., and Heather A. Clark, "*Conserved arginine-516 of Penicillium amagasakiense glucose oxidase is essential for the efficient binding of  $\beta$ -D-glucose*," BIOCHEMICAL JOURNAL, vol. 347, no. 2, pp. 553-559, **2000**.
- [53] V. Leskovac, S. Trivić and G. Wohlfahrt, "*Glucose oxidase from Aspergillus niger: the mechanism of action with molecular oxygen, quinones, and one-electron acceptors*," The International Journal of Biochemistry & Cell Biology, vol. 37, p. 731–750, **2005**.
- [54] S. Witt, M. Singh and H. M. Kalisz, "*Structural and Kinetic Properties of Nonglycosylated Recombinant Penicillium amagasakiense Glucose Oxidase Expressed in Escherichia coli*," Applied and Environmental Microbiology, vol. 64, no. 4, pp. 1405-1411, **1998**.
- [55] H. Bergmeyer, M. Horder and R. Rej, "*International-federation-of-clinical-chemistry-scientific committee analytical section expert panel on enzymes*," Clinical Chemistry and Laboratory Medicine, vol. 24, no. 7, p. 481–510, **1986**.
- [56] V. A. Alferov, M. G. Zaitsev and O. N. Ponomareva, "*Functional nanofiber mat of polyvinyl alcohol/gelatin containing nanoparticles of biphasic calcium phosphate for bone regeneration in rat calvaria defects*" Journal of Analytical Chemistry, vol. 66, no. 12, p. 1205–1211, **2011**.
- [57] P. Goswami, S. S. R and Chinnadayala, "*An overview on alcohol oxidases and their potential applications*," Applied Microbiological Biotechnology, vol. 97, p. 4259–4275, **2013**.
- [58] H. B. Yildiz and L. Toppare, "*Biosensing approach for alcohol determination using immobilized alcohol oxidase*," Biosensors and Bioelectronics, vol. 21, p. 2306–2310, **2006**.
- [59] B. Kuswandi, T. Irmawati and M. A. Hidayat, "*A Simple Visual Ethanol Biosensor Based on Alcohol Oxidase Immobilized onto Polyaniline Film for Halal Verification of Fermented Beverage Samples*," Sensors, vol. 14, pp. 2135-2149, **2014**.
- [60] M. I. Baker, S. P. Walsh and Z. Schwartz, "*A review of polyvinyl alcohol and its uses in cartilage and orthopedic applications*," Biomedical Materials Research-Part B, vol. 100, p. 1451–1457, **2012**.

- [61] C. M. Wong, & K. H. Wong and & X. D. Chen, "*Glucose oxidase: natural occurrence, function, properties and industrial applications*," Applied Microbiological Biotechnology, vol. 78, p. 927–938, **2008**.
- [62] A. Amanda and S. K. Mallapragada, "*Comparison of Protein Fouling on Heat-Treated Poly(vinyl alcohol), Poly(ether sulfone) and Regenerated Cellulose Membranes Using Diffuse Reflectance Infrared Fourier Transform Spectroscopy*," Biotechnology Progress, vol. 17, p. 917–923, **2001**.
- [63] J. M. Gohil, A. Bhattacharya and P. Ray, "*Studies on the Cross-linking of Poly(Vinyl Alcohol)*," Journal of Polymer Research, vol. 13, p. 161–169, **2006**.
- [64] K. C. S. Figueiredo and T. L. M. Alves, "*Poly(vinyl alcohol) Films Crosslinked by Glutaraldehyde Under Mild Conditions*," Journal of Applied Polymer Science, vol. 111, p. 3074–3080, **2009**.
- [65] D. T. Pierce, P. R. and A. J. Bard, "*Scanning Electrochemical Microscopy. 17. Studies of Enzyme-Mediator Kinetics for Membrane- and Surface-Immobilized Glucose Oxidase*," Analytical Chemistry, vol. 64, pp. 1795-1804, **1992**.
- [66] A. J. Bard, F.-R. F. Fan and J. Kwak, "*Scanning Electrochemical Microscopy. Introduction and Principles*," Analytical Chemistry, vol. 61, pp. 132-138, **1989**.
- [67] C. E. Banks, T. J. Davies and G. G. Wildgoose, "*Electrocatalysis at graphite and carbon nanotube modified electrodes: edge-plane sites and tube ends are the reactive sites*," Chemical Communications, vol. 7, pp. 829-841, **2005**.
- [68] T. J. Davies, M. E. Hyde and R. G. Compton, "*Nanotrench Arrays Reveal Insight into Graphite Electrochemistry*," Angewandte Chemie-International Edition, vol. 44, p. 5121 –5126, **2005**.
- [69] T. S. Miller, N. Ebejer and A. G. Güell, "*Electrochemistry at carbon nanotube forests: sidewalls and closed ends allow fast electron transfer*," Chemical Communication, vol. 48, pp. 7435-7437, **2012**.
- [70] G. Ren, X. Xu, J. C. Qiang Liu, X. Yuan, L. Wu and Y. Wan, "*Electrospun poly(vinyl alcohol)/glucose oxidase biocomposite membranes for biosensor applications*," Reactive and Functional Polymers, vol. 66, p. 1559–1564, **2006**.
- [71] Q. P. PHAM, U. SHARMA and A. G. MIKOS, "*Electrospinning of Polymeric Nanofibers for Tissue Engineering Applications: A Review*," TISSUE ENGINEERING, vol. 12, no. 5, pp. 1197-1211, **2005**.

# CURRICULUM VITAE

## Personal Information

Name and Surname: ANAERGULI MAIHEMUTI

Place of Birth: Yenihisar/Kashgar

Social status: Married

E-mail: anargulmahmud@gmail.com

Adress : Koruturk mah. Izmir/Turkey

## Education

Undergraduate: Shanghai University of Engineering and Technology, school of Pharmacy Engineering

## Foreign Languages and levels

Chinese(advanced)

English(advanced)

Turkish(advanced)

## Work Expeirence

Volunteer in Shanghai Expo 2010.

## Experience fields

Research Assistant at Shanghai Pharmaceutical Research Centre. Determination of  $\beta$  -Sitosterol with Chemical Course and Material Applications in Jatropha Seed Oil by High Performance Liquid Chromatography. It has been published on Nanoscience and Nanomaterials.

## Publication

"Determination of  $\beta$  -Sitosterol with Chemical Course and Material Applications in Jatropha Seed Oil by High Performance Liquid Chromatography"



HACETTEPE ÜNİVERSİTESİ  
FEN BİLİMLERİ ENSTİTÜSÜ  
YÜKSEK LİSANS TEZ ÇALIŞMASI ORJİNALLİK RAPORU

HACETTEPE ÜNİVERSİTESİ  
FEN BİLİMLER ENSTİTÜSÜ  
NANOTEKNOLOJİ VE NANOTİP ANABİLİM DALI BAŞKANLIĞI'NA

Tarih: 1.6.2018

Tez Başlığı / Konusu: Organik Moleküllerin Tayini için Nanofiber Bazlı Elektrotların Kullanımı

Yukarıda başlığı/konusu gösterilen tez çalışmamın a) Kapak sayfası, b) Giriş, c) Ana bölümler d) Sonuç kısımlarından oluşan toplam 65 sayfalık kısmına ilişkin, 18/05/2018 tarihinde tez danışmanım tarafından Turnitin adlı intihal tespit programından aşağıda belirtilen filtrelemeler uygulanarak alınmış olan orjinallik raporuna göre, tezin benzerlik oranı % 9 'dur.

Uygulanan filtrelemeler:

- 1- Kaynakça hariç
- 2- Alıntılar hariç
- 3- 5 kelimedenden daha az örtüşme içeren metin kısımları hariç

Hacettepe Üniversitesi Fen Bilimleri Enstitüsü Tez Çalışması Orjinallik Raporu Alınması ve Kullanılması Uygulama Esasları'nı inceledim ve bu Uygulama Esasları'nda belirtilen azami benzerlik oranlarına göre tez çalışmamın herhangi bir intihal içermediğini; aksinin tespit edileceği muhtemel durumda doğabilecek her türlü hukuki sorumluluğu kabul ettiğimi ve yukarıda vermiş olduğum bilgilerin doğru olduğunu beyan ederim.

Gereğini saygılarımla arz ederim.

Tarih ve İmza

Adı Soyadı: ANAERGULI MAIHEMUTİ  
Öğrenci No: N13121239  
Anabilim Dalı: NANOTEKNOLOJİ VE NANOTİP  
Programı: -  
Statüsü:  Y.Lisans  Doktora  Bütünleşik Dr.

1.6.2018

**DANIŞMAN ONAYI**

UYGUNDUR.

PROF. DR. NECDET SAĞLAM  
(Unvan, Ad Soyad, İmza)



## YAYINLAMA VE FİKRİ MÜLKİYET HAKLARI BEYANI

Enstitü tarafından onaylanan lisansüstü tezinin/raporumun tamamını veya herhangi bir kısmını, basılı (kağıt) ve elektronik formatta arşivleme ve aşağıda verilen koşullarla kullanıma açma iznini Hacettepe üniversitesine verdiğimi bildiririm. Bu izinle Üniversiteye verilen kullanım hakları dışındaki tüm fikri mülkiyet haklarım bende kalacak, tezinin tamamının ya da bir bölümünün gelecekteki çalışmalarda (makale, kitap, lisans ve patent vb.) kullanım hakları bana ait olacaktır.

Tezin kendi orijinal çalışmam olduğunu, başkalarının haklarını ihlal etmediğimi ve tezinin tek yetkili sahibi olduğumu beyan ve taahhüt ederim. Tezimde yer alan telif hakkı bulunan ve sahiplerinden yazılı izin alınarak kullanması zorunlu metinlerin yazılı izin alarak kullandığımı ve istenildiğinde suretlerini Üniversiteye teslim etmeyi taahhüt ederim.

- Tezinin/Raporumun tamamı dünya çapında erişime açılabilir ve bir kısmı veya tamamının fotokopisi alınabilir.**  
(Bu seçenekle teziniz arama motorlarında indekslenebilecek, daha sonra tezinizin erişim statüsünün değiştirilmesini talep etmeniz ve kütüphane bu talebinizi yerine getirirse bile, tezinin arama motorlarının önbelleklerinde kalmaya devam edebilecektir.)
- Tezinin/Raporumun ..... tarihine kadar erişime açılmasını ve fotokopi alınmasını (İç Kapak, Özet, İçindekiler ve Kaynakça hariç) istemiyorum.**  
(Bu sürenin sonunda uzatma için başvuruda bulunmadığım takdirde, tezinin/raporumun tamamı her yerden erişime açılabilir, kaynak gösterilmek şartıyla bir kısmı ve ya tamamının fotokopisi alınabilir)
- Tezinin/Raporumun ..... tarihine kadar erişime açılmasını istemiyorum, ancak kaynak gösterilmek şartıyla bir kısmı veya tamamının fotokopisinin alınmasını onaylıyorum.**
- Serbest Seçenek/Yazarın Seçimi**

19 / 06 / 2018

ANAERGULI MAIHEMUTİ